



**NTNU – Trondheim**  
Norwegian University of  
Science and Technology

# Control Oriented Modelling of a Steam Cycle

**Ida Andersskog**

Submission date: December 19, 2018  
Supervisor: Prof Sigurd Skogestad, IKP  
Co-Supervisor: Cristina Zotica, IKP

Norwegian University of Science and Technology  
Department of Chemical Engineering

# Abstract

The first objective for this project was to model a power generating steam cycle in Simulink. The second objective was to study if the liquid holdup in the boiler could be used as an energy storage item to vary the power output for small periods of time. This was done by proposing a control structure of the steam cycle model, and by introducing step responses in the inputs, to see how the dynamics in the holdup could be used to regulate these variations and within what limitations this can be done.

The steam cycle modelled consist of a boiler, super-heater, attemperator, high pressure turbine, reheater, low pressure turbine, condenser and a pump. Problems in the modelling of the mass flows by the linear valve equation lead to accumulation in the liquid holdup in the boiler and thus no proper steady state model was found for  $M_1$  at design conditions. It was however possible to tune and verify a level controller for  $M_1$ , but the poor approximation of  $\dot{m}_2$  caused problems in the simulations at large variations. The temperature controller of  $T_2$  was found to require a larger controller gain to obtain acceptable temperature control.

The Stodola approximation of the turbine flow was found to tolerate variations in the system better than using the constant volumetric flow approximation.

The large liquid holdup before the turbine,  $M_{turbine}$ , slowed down the dynamics in the system and gave smooth responses, but also low sensitivity to the speed of the level controller. Indications show that an increase in the valve position,  $z$ , combined with a level controller for the boiler could be used to produce higher power output for a short period of time. The aim of utilizing the liquid holdup as an energy storage cannot be concluded directly until better modelling is made. These improvements should be made specifically with regards to the flow out of the boiler, pressure out of the turbine as well better coupling within the system flows and the resulting dynamics of the holdups in the system.

The variations in the flue gas was found to be limited by +1% and -10% caused by convergence problems as well as too low temperature at the turbine outlet.



# Preface

This report is submitted as a result of the specialization project for the process systems engineering group at the Norwegian University of Science and Technology during autumn 2018. I would like to thank my supervisor Prof. Sigurd Skogestad and co-supervisor Cristina Zotica for their support, discussion and engagement throughout the project.



# Contents

<b>1</b>	<b>Introduction</b>	<b>1</b>
1.1	Report structure . . . . .	2
<b>2</b>	<b>Theory</b>	<b>3</b>
2.1	Steam cycle power plant . . . . .	3
2.1.1	Boiler . . . . .	3
2.1.2	Turbine . . . . .	5
2.1.3	Super-heater . . . . .	6
2.2	Dynamic conservation balances . . . . .	6
2.3	Simulink . . . . .	7
2.3.1	DAE . . . . .	8
2.3.2	ODE . . . . .	8
2.3.3	AE . . . . .	9
2.4	Pressure - flow network model . . . . .	10
2.5	PID control . . . . .	10
2.5.1	SIMC - tuning . . . . .	11
<b>3</b>	<b>Modelling of the steam cycle</b>	<b>15</b>
3.1	Assumptions . . . . .	15
3.2	Model representation . . . . .	16
3.3	States . . . . .	18
3.4	Steam cycle power plant . . . . .	18
3.4.1	Boiler . . . . .	18
3.4.2	Superheater . . . . .	19
3.4.3	Heat exchangers . . . . .	19
3.4.4	Attemperator . . . . .	20
3.4.5	Turbine . . . . .	20
3.4.6	Condenser . . . . .	22
3.4.7	Pump and valves . . . . .	23
3.5	Control structure . . . . .	24
3.5.1	MVs, CVs and DVs . . . . .	24
3.5.2	Proposed control pairings . . . . .	25
3.5.3	Controller tuning . . . . .	28

<b>4</b>	<b>Simulation</b>	<b>29</b>
4.1	Stability of simulation . . . . .	29
4.2	Stodola vs Constant volumetric flow . . . . .	30
4.3	Open loop responses without holdup control . . . . .	32
4.3.1	10% increase in inlet flow, $\dot{m}_1$ . . . . .	32
4.3.2	10% increase in bypass flow, $\dot{m}_{bypass}$ . . . . .	33
4.3.3	10% increase in valve position, $z$ . . . . .	34
4.3.4	Variation of flue gas flow, $\dot{m}_G$ in the heat exchanger . . . . .	35
4.4	Step responses with the holdup and temperature controllers active . . .	37
4.4.1	Closed loop 10% setpoint change $M_{1s}$ . . . . .	38
4.4.2	Closed loop 10% setpoint change in $T_{2s}$ . . . . .	39
4.4.3	10% step increase in the valve position, $z$ . . . . .	41
4.4.4	Variation fo the flue gas flow, $\dot{m}_G$ in the heat exchanger . . . . .	44
<b>5</b>	<b>Discussion and further recommendations</b>	<b>47</b>
<b>6</b>	<b>Conclusion</b>	<b>51</b>
<b>A</b>	<b>Appendix</b>	<b>55</b>
A.1	Units . . . . .	55
A.2	Parameters . . . . .	56
A.3	Steady state data and nominal values . . . . .	57
A.4	Setpoints for the PID controllers . . . . .	58
A.5	Step responses for tuning of controller . . . . .	59
A.5.1	Holdup controller of $M_1$ . . . . .	59
A.5.2	Temperature controller of $T_2$ . . . . .	61
A.5.3	Temperature controller of $T_{3mid}$ . . . . .	62
A.5.4	Temperature controller of $T_4$ . . . . .	63
A.5.5	Pressure controller of $P_1$ . . . . .	64
A.5.6	Power controller of $W_s$ . . . . .	65
A.6	Step responses with holdup control (MC) . . . . .	66
A.6.1	Increase in bypass flow . . . . .	66
A.6.2	Variation of valve position . . . . .	67
A.6.3	Variation of flue gas flow in HEX . . . . .	69
A.7	Figure of the Simulink model . . . . .	71

# List of Figures

1.1	Figure representing a simple Rankine cycle . . . . .	1
2.1	Process flow diagram for a simple steam cycle . . . . .	4
2.2	A representation of the DAE system model in Simulink . . . . .	9
2.3	Pressure Nodes and Flow Elements for the open steam cycle . . . . .	10
2.4	Example plot of a steady state step response . . . . .	12
2.5	Example plot of an integrating step response . . . . .	12
3.1	Process flow diagram for the steam cycle . . . . .	16
3.2	Process flow diagram for the modeled turbine subsystem . . . . .	17
3.3	Process flow diagram of the steam cycle with the proposed control structure	27
3.4	Process flow diagram of the turbine subsystem with the proposed control structure . . . . .	27
3.5	Example of how to model PID-control in Simulink . . . . .	28
4.1	Plot of the liquid holdups and flows for the boiler, attemperator and turbine at design conditions with no control . . . . .	29
4.2	Plot of the most important variables at steady state using constant volumetric flow . . . . .	30
4.3	Plot of the most important variables at steady state using Stodolas Equation	30
4.4	Plot of a 10% step on $z$ when using the constant volumetric flow approximation . . . . .	31
4.5	Plot of a 10% step on $z$ when using the Stodola equation approximation .	31
4.6	Plot of the response on $M_1$ after a 10% step of $\dot{m}_1$ . . . . .	32
4.7	Plot of the response after a 10% step of $\dot{m}_{bypass}$ . . . . .	33
4.8	Plot of the response after a 10% step of $z$ . . . . .	34
4.9	Plot of the response after a 1% step of $\dot{m}_G$ . . . . .	35
4.10	Plot of the response after a -10% step of $\dot{m}_G$ . . . . .	36
4.11	Plot of the response after a 10% setpoint change of $M_1$ . . . . .	38
4.12	Plot of the response in $W_s$ after a 10% setpoint change of $M_1$ . . . . .	38
4.13	Plot of the response after a 10% change in the setpoint of $T_2$ . . . . .	39
4.14	Plot of the response in $W_s$ after a 10% change in the setpoint of $T_2$ . .	39

4.15	Plot of the response after a 10% change in the setpoint of $T_2$ . $K_{cbypass} = -1.0820$ . . . . .	40
4.16	Plot of the response in $W_s$ after a 10% change in the setpoint of $T_2$ . $K_{cbypass} = -1.0820$ . . . . .	40
4.17	Plot of the response after a 10% step of $z$ with MC and TCs on. $K_{c1} = 14.64$ . . . . .	41
4.18	Plot of the response after a 10% step of $z$ with MC and TCs on. $K_{c1} = 0.1464$ . . . . .	42
4.19	Plot of the response after a 10% step of $z$ with MC and TCs on. $K_{c1} = 0.01464$ . . . . .	43
4.20	Plot of the response after a 10% step of $z$ with MC and TCs on . . . . .	43
4.21	Plot of the response after a 1% step of $\dot{m}_G$ with MC and TCs on. $K_{c1} = 0.1464$ . . . . .	44
4.22	Plot of the response after a -10% step of $\dot{m}_G$ with MC and TCs on. $K_{c1} = 0.1464$ . . . . .	45
A.1	Plot of $M_1$ and $\dot{m}_1$ after a 10% open loop step response in $\dot{m}_1$ . . . . .	59
A.2	Plot of $M_1$ and $\dot{m}_1$ after a 10% closed loop setpoint changer in $M_{1s}$ . $K_{c1} = 0.1465$ . . . . .	60
A.3	Plot of $T_2$ and $\dot{m}_{bypass}$ after a 10% open loop step response in $\dot{m}_{bypass}$ . . . . .	61
A.4	Plot of $T_2$ and $\dot{m}_{bypass}$ after a 10% closed loop setpoint change in $T_{2s}$ . $K_{cbypass} = -0.1082$ . . . . .	61
A.5	Plot of $T_{3mid}$ and $\dot{m}_{G2}$ after a 10% open loop step response in $\dot{m}_{mG}$ . . . . .	62
A.6	Plot of $T_{3mid}$ and $\dot{m}_{G2}$ after a 10% closed loop setpoint change in $T_{3mids}$ . $K_{cReheater} = 0.28$ . . . . .	62
A.7	Plot of $T_4$ and $Q_c$ after a 10% open loop step response in $Q_c$ . . . . .	63
A.8	Plot of $T_4$ and $Q_c$ after a 10% closed loop closed loop setpoint change in $T_{4s}$ . $K_{cQc} = 1.9843e6$ . . . . .	63
A.9	Plot of $P_1$ and $z$ after a 10% open loop step response in $z$ . . . . .	64
A.10	Plot of $P_1$ and $z$ after a 10% closed loop setpoint change in $P_{1s}$ . $K_{cz} = -6.8538e-06$ , $\tau_{Iz} = 3$ . . . . .	64
A.11	Plot of $W_s$ and $\dot{m}_G$ after a 1% open loop step response in $\dot{m}_G$ . . . . .	65
A.12	Plot of $W_s$ and $\dot{m}_G$ after a 1% closed loop setpoint change in $W_{ss}$ . $K_{cW_s} = -2.1620e-7$ . . . . .	65
A.13	Plot of the response after a 10% step of $\dot{m}_{bypass}$ with MC on . . . . .	66
A.14	Plot of the response after a 10% step of $z$ with MC on. $K_{c1} = 0.1465$ . . . . .	67
A.15	Plot of the response after a 10% step of $z$ with MC on. $K_{c1} = 1.465$ . . . . .	67
A.16	Plot of the response after a 10% step of $z$ with MC on. $K_{c1} = 14.65$ . . . . .	68
A.17	Plot of the response after a 1% step of $\dot{m}_G$ with MC on. $K_{c1} = 0.1465$ . . . . .	69
A.18	Plot of the response after a 1% step of $\dot{m}_G$ with MC on. $K_{c1} = 14.65$ . . . . .	69
A.19	Plot of the response after a -10% step of $\dot{m}_G$ with MC on. $K_{c1} = 0.1465$ . . . . .	70
A.20	Screen-shot of the steam cycle Simulink model part 1 . . . . .	71
A.21	Screen-shot of the steam cycle Simulink model part 2 . . . . .	72

A.22 Screen-shot of the steam cycle Simulink model part 3 . . . . .	73
A.23 Screen-shot of the steam cycle Simulink model part 4 . . . . .	74



# Abbreviations

The next list describes several abbreviations that will be later used within the body of the document

AE	Algebraic equation
CV	Controlled variable
DAE	Differential algebraic equations
DOF	Degrees of freedom
DV	Disturbance variable
HEX	Heat exchanger
HP	High pressure
LP	Low pressure
MC	Holdup (mass) controller
MV	Manipulated variable
ODE	Ordinary differential equations
PC	Pressure controller
PID	Predictive-Integrating-Derivative
PowerC	Power controller
SIMC	Simplified/Skogestad - Internal-Model-Control
TC	Temperature controller
UA	Heat transfer coefficient multiplied with the surface area where the heat transfer takes place



# 1 — Introduction

A Rankine cycle is a thermodynamic cycle that converts thermal energy into mechanical energy by use of phase change through an energy carrier medium. The thermal energy is supplied to the medium externally and the Rankine cycle is therefore widely used to predict the performance when utilizing heat from nuclear plants, waste and fossil fuel combustion through steam turbine systems. Represented in the process flow diagram in Figure 1.1 is a simple Rankine cycle. It consists of four main processes. The first is evaporation in the boiler by addition of heat, where the steam generated is expanded through the turbine process. The expanded steam is further condensed in the next step by a cooler and sent back to the cycle through a pump that boosts the liquid pressure. Utilization of the heat can be done through an steam cycle that converts the mechanical energy through the turbine blades to electrical energy through a generator. (Kovacs, 2004-2014) The Rankine cycle can be therefore considered an idealized version of the steam cycle.

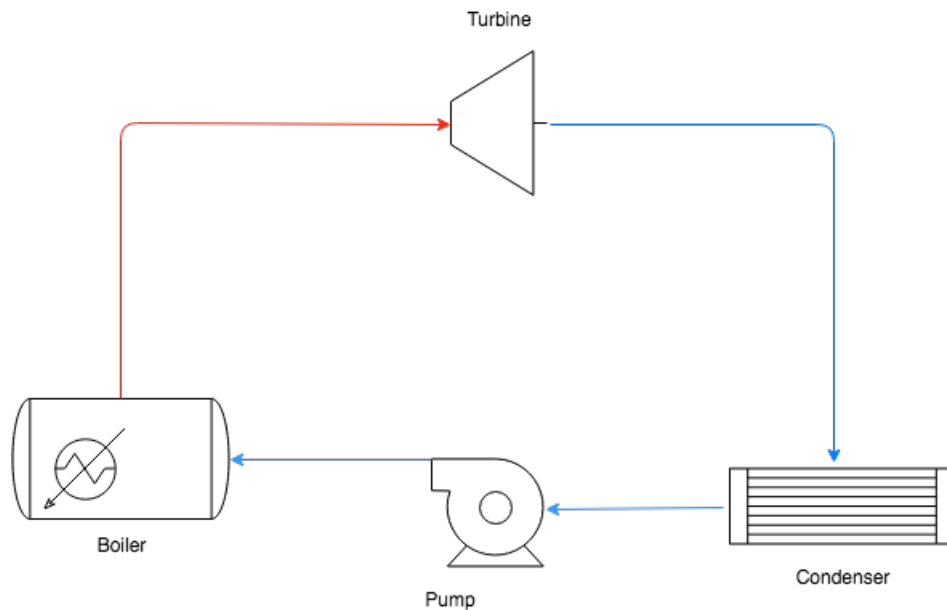


**Figure 1.1:** Figure representing a simple Rankine cycle

In this project the first objective is to model the steam cycle in the simulation environment Simulink. Simulink is a block-based simulation environment that combined with the program MATLAB can be used to model a system by both code and graphical interface. The blocks in Simulink allows for the separation of sub-processes in a system with the use of subsystem blocks. The subsystems created in the steam cycle model was inspired from the process flow diagram and consisted of a boiler, superheater, attemperator, turbine, condenser and pump subsystem. The turbine subsystem had lower layer subsystems that included a valve, buffer tank (liquid holdup), HP turbine, reheater and LP turbine subsystem.

The current modelling of power generating steam cycles is mainly focused on improving the overall efficiency and power production.(Alobaid F. and B., 2017) It is done primarily with regards to implementation of co-generation power plants, addition of turbines, heating elements and improvement of turbine component materials.(Oryds A.W and M.J, 1994)(Kovacs, 2004-2014) This project is a part of SINTEFs highEFF project which is about increasing energy efficiency for a greener industry. One of the aims of the highEFF project is to increase energy efficiency of the components within energy production processes. As the power demand in the market may fluctuate it is desired to see if liquid holdups or buffer tanks can be used to vary the power output for small periods of time as if the buffer tanks act as an energy storage. Accordingly, the second objective of this project is to see how the liquid holdup in the boiler affects the power output, if it can act as an energy storage item and within what limitations.

### 1.1 Report structure

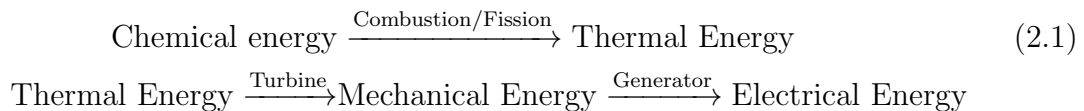
- Chapter 2 introduces the reader to the necessary theory behind the steam cycle power plant, its model equations, the simulation tools and models used as well as the PID control method and SIMC tuning.
- Chapter 3 presents the assumptions, model representation, states, inputs, specific subsystem modelling and a proposed control structure for the steam cycle.
- Chapter 4 contain plots of the various simulation results of the modelled steam cycle.
- Chapter 5 discusses the results and proposes further recommendations in the model.
- Chapter 6 concludes the overall project

## 2 — Theory

### 2.1 Steam cycle power plant

Power plants can be classified into thermal-, electrical- or co-energy production power plants. Most of the power plants have a co-energy production that produces both thermal energy in the form of steam production and district heating, as well as electricity. (Kovacs, 2004-2014) In this project an electrical power plant is assumed for simplicity.

Within the power plant itself there are several energy carriers which transports the energy. The primary, used as the heating source, is classified into non-renewable and renewable sources, where most of the renewable energy sources convert their energy directly into electrical energy. The energy carrier in the case of heating steam is required to undergo thermal and mechanical energy transfer as represented in Equation 2.1.



Appropriate primary energy carriers used in a steam cycle is consequently fossil fuels, nuclear, waste and biomass. The secondary energy carrier is in this case the water/steam. (Kovacs, 2004-2014, p.27)

The cycle can be divided into several important main components as represented in Figure 2.1. The most important dynamics are found in the boiler. For this reason, most advancements within the modelling will be for the boiler.

#### 2.1.1 Boiler

In the boiler water is heated until it reaches the point at which it vaporizes and steam is generated. Kovacs (2004-2014) At normal pressures around 1.013 Bar ( $1.1013 \cdot 10^5 \text{Pa}$ ) the boiling point is at 373.15K (100°C). (Skogestad, 2009, p.341)

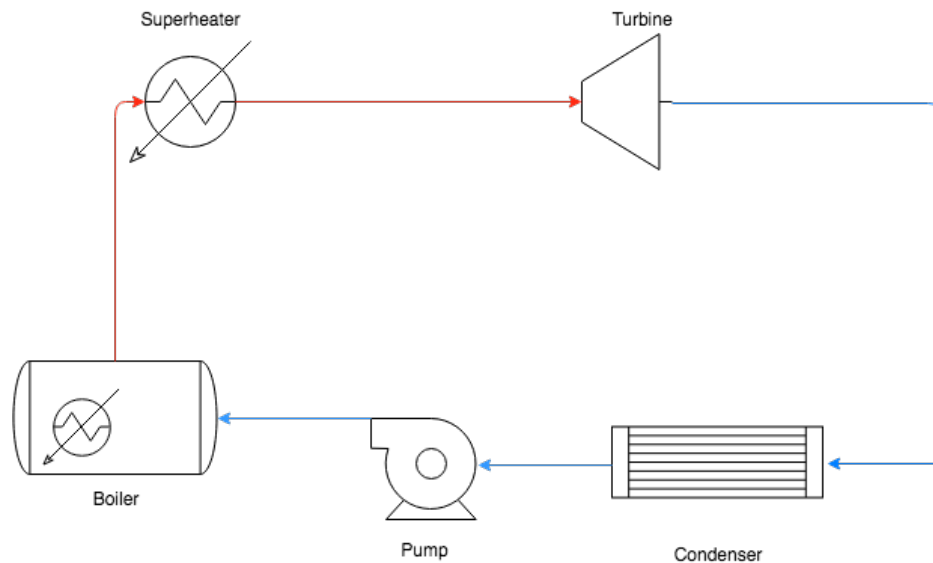


**Figure 2.1:** Process flow diagram for a simple steam cycle

A high pressure and temperature is desired for the steam sent into the turbine. This is because a high temperature and pressure means increased enthalpy and pressure drop over the turbine and thus more power is generated.

The steam out of the boiler is saturated, hence, the saturation pressure will need to be computed. A widely used saturation pressure equation is the Antoine Equation. The Antoine equation describes a semi-empirical correlation between saturated pressure and temperature for pure components by the use of three constants: A, B and C. (Skogestad, 2009, p.342)

$$\log_p = A - \frac{B + T}{C} \quad (2.2)$$

The Antoine constants for calculation of the saturation pressure of water in Bar is rendered in Table 2.1 below.

Constant	Value
A	11.6834
B	3816.44
C	-46.13

**Table 2.1:** Antoine constant for saturated steam

## 2.1.2 Turbine

A steam turbine is a component that converts the kinetic energy in the high pressure steam to mechanical energy by the use of rotor blades. The mechanical energy from the axial rotation of these blades is then converted to electrical energy through a generator. (Alobaid F. and B., 2017)

The expansion of the steam through the turbine system can be controlled by addition of valves and extraction points between the turbines. Uncontrolled expansions are thus turbines where the in and outlet pressure or flow is not regulated which leads the pressure ratio over the turbine to vary. (Cooke, 1985)

### Constant volumetric flow

For uncontrolled expansions to high vacuum, the mass flow through the turbine can be computed by assuming a constant volumetric flow rate. This leads a linear relation by the use of the ideal gas law as shown in Equation 2.3. (Cooke, 1985, p.598)

$$\dot{m}_{turbine} = q_{3s} \frac{M_{m,water} P_3}{RT_3} \quad (2.3)$$

where the volumetric flow constant,  $q_{3s}$  can be computed at the initial (design) conditions for the flow,  $\dot{m}_{turbine}^0$  and inlet temperature,  $T_3^0$ .

### Stodola Equation

As the mass flow rate and the pressure may vary during the simulation (off-design conditions), constant volumetric flow might not predict the flow through the turbine accurately at off-design conditions. (Cooke, 1985, p.598-599) Hence, another relation represented by the Stodola Equation is introduced in determining the performance of the turbine as shown in Equation 2.4. (Cooke, 1985) (Mazzi N. and A., 2015)

$$\dot{m}_{in} = K_t \sqrt{\rho_{in} P_{in} \left[ 1 - \left( \frac{P_{out}}{P_{in}} \right)^2 \right]} \quad (2.4)$$

where the Stodola coefficient,  $K_t$ , is found from nominal values by Equation 2.5.

$$K_t = \frac{\dot{m}_{in,nom}}{\sqrt{\rho_{in,nom} P_{in,nom} \left[ 1 - \left( \frac{P_{out,nom}}{P_{in,nom}} \right)^2 \right]}} \quad (2.5)$$

The Stodola Equation should only be applied to single staged turbines if the expansion ratio is constant. (Cooke, 1985) For expansions with high pressure change and outlet

pressures close to vacuum more stages are needed. This is done by adding additional turbines with smaller expansion ratios such as for example a high pressure turbine followed by a low pressure turbine. This decreases the pressure loads on the individual turbine and allows for the addition of a reheater in between the turbine. Thus the risk of steam condensation through the turbine is minimized. (R. and G., p. 121)

### 2.1.3 Super-heater

The concept of super-heating the steam is to obtain a higher efficiency of the steam cycle. Superheating steam increases the kinetic energy of the steam and thus more power can be produced. Another important aspect of heating the steam is to minimize the risk of condensation through the turbine as water will cause erosion and thus damage the turbine. For systems with more than one turbine, a reheater can also help minimizing this risk, but here only superheating the steam will be necessary for the high and intermediate pressure turbines. (Skogestad, 2009, p.194) There exists limitations on how much the steam can be heated with regards to the material of the turbine blades themselves. At a certain point the material in the blades starts to melt and thus the turbine will be damaged. The highest steam conditions possible up to today is about 620 °C. (P., 2012)

## 2.2 Dynamic conservation balances

Dynamic conservation of mass and energy is represented by ordinary differential equations for the respected physical systems. (D.M. and J.B., 2012)

Assuming no chemical reactions in the system, the dynamic state of mass,  $M$ , is simply represented in terms of accumulation over time by the difference in the in and out flows,  $\dot{m}_{in}$  and  $\dot{m}_{out}$  of the system as shown in Equation 2.6.

$$\frac{dM}{dt} = \dot{m}_{in} - \dot{m}_{out} \quad (2.6)$$

The conservation of energy is done through a simplified dynamic energy balance by assuming constant heat capacity,  $C_p$ . The dynamic state in this case is the enthalpy,  $H$ , of the total system, and is represented in Equation 2.7.

$$\frac{dH}{dt} = \dot{m}_{in}h_{in} - \dot{m}_{out}h_{out} + \dot{Q} \quad (2.7)$$

Where the specific enthalpy,  $h$ , has to be calculated from its reference state with the respected heat capacity,  $C_p$ , and possible phase changes accounted for as represented in Equation 2.8 with the added enthalpy of vaporization in the case of phase change from liquid to gaseous state.

$$h(T) = C_p(T - T_{ref}) + \Delta H_{vap}(T_{ref}) \quad (2.8)$$

Combining Equation 2.6 and Equation 2.7 produces a variation of the energy balance on the form of temperature as shown in Equation 2.9.

$$\frac{dT}{dt} = \frac{1}{M} \left( \dot{m}_{in}(h_{in} - h) - \dot{m}_{out}(h_{out} - h) + \dot{Q} - \dot{h} \right) \quad (2.9)$$

Where the heat transfer,  $Q$ , by convection can be computed from its heat coefficient through the empirical formula for convection as shown in Equation 2.10.

$$\dot{Q} = -UA\Delta T \quad (2.10)$$

The temperature difference,  $\Delta T$ , in heat exchangers is normally approximated through the logarithmic mean,  $\Delta T_{lm}$ . If the enthalpy is modelled on its temperature form, the logarithmic mean can be difficult to integrate. Thus, a simplified arithmetical mean will be used when modelling the convection through the heat exchanger:

$$\Delta T = \left( \frac{T_{in,hot} + T_{out,hot}}{2} \right) - \left( \frac{T_{in,cold} + T_{out,cold}}{2} \right) \quad (2.11)$$

The work,  $W_s$ , is modelled as an isentropic expansion where the pressure ratio is the basis for its computation as shown in Equation 2.13. (Skogestad, 2009, p. 141,201-202)

$$T_{out} = T_{in} \left( \frac{P_{in}}{P_{out}} \right)^{\frac{R}{C_p}} \quad (2.12)$$

$$W = \dot{m}C_p(T_{out} - T_{in}) \quad (2.13)$$

## 2.3 Simulink

Simulink is a block based simulation environment that, combined with MATLAB, can be used to design a simulation with both text-code and graphical programming. In Simulink the user can utilize several system blocks such as the MATLAB function block, solver blocks and subsystem blocks, that will lower the amount of code needed to be written by hand. (The MathWorks, 2018c)

The subsystem blocks allows for grid - like separation of the process components by modelling them in their own subsystem. By doing so an external user can directly look at the simulation from a front end point of view as if it was a process flow diagram. To get more details about the desired subsystem the user can click into the subsystems to see how the component is modelled and then further go into the specific function blocks in MATLAB to see the function code.

Inside the subsystem blocks there are various model functions to obtain the desired dynamic and algebraic states. In this project a clear separation of the function systems has been made as the various subsystems contain different types of states and functions.

### 2.3.1 DAE

Differential algebraic equations (DAE) is a set of dynamic and algebraic systems where the dynamic and algebraic states are computed together to obtain the final solution. A representation of a semi-explicit DAE is shown in Figure 2.14.

$$\frac{dx}{dt} = f_1(x, z, u) \quad (2.14)$$

$$0 = f_2(x, z, u) \quad (2.15)$$

Where  $x$  is the dynamic state,  $u$  the input and  $z$  the algebraic state. (The MathWorks, 2018a) It can be represented with a single MATLAB function in Simulink and the dynamic and algebraic states become separated but solved simultaneously as shown in Figure 2.2. (The MathWorks, 2018b) The separation of the states are done by the use of the gain block in Simulink.

A non-square selection matrix is used as a gain,  $K$ . The structure of  $K$  for the differential equations consists of a  $[N_d \times N_{eq}]$  matrix with 1 on the position of the column that corresponds to the equation used to compute the dynamic state and 0 for the rest. The structure of  $K$  for the algebraic equation consist of a  $[N_a \times N_{eq}]$  with 1 on the position of the column that corresponds to the equation used to compute the algebraic state and 0 for the rest.  $N_d$  is the number of differential equations,  $N_a$  is the number of algebraic equations and  $N_{eq}$  is the total number of equations.

### 2.3.2 ODE

Ordinary differential equations (ODE) represents a straight dynamic system, where the dynamic state can be solved by integration of its differential form.

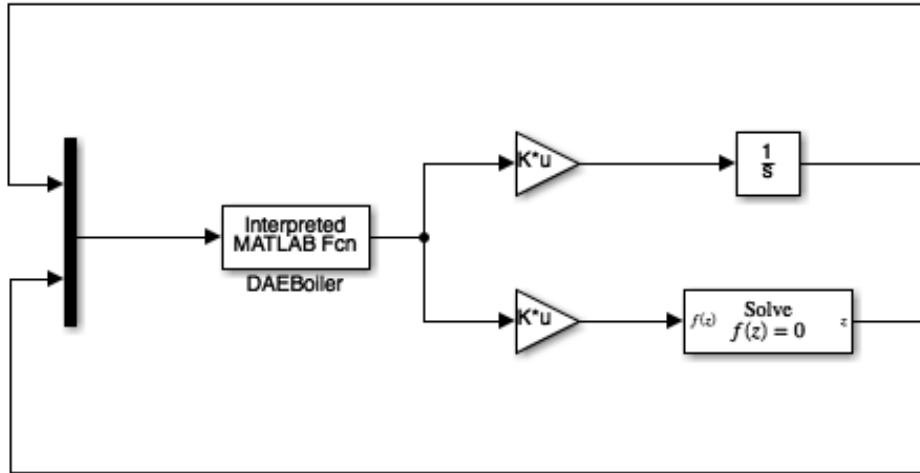


**Figure 2.2:** A representation of the DAE system model in Simulink

$$\frac{dx}{dt} = f(x, z, u) \quad (2.16)$$

An ODE can be modelled in Simulink by the use of a MATLAB function block and an integrator where the dynamic state is looped back into the function until convergence.

### 2.3.3 AE

Algebraic equations (AE) are functions that takes in the inputs, state variables and parameters and computes the algebraic state. The algebraic equations have been solved with two different methods in this project. The first method builds on the same implementation as shown in Section 2.3.1, by setting the equation on a form that equals a constant (or zero) value and solving it by iteration until converges to compute the algebraic state.

$$0 = f(x, z, u) \quad (2.17)$$

This method should be used when there are a set of algebraic equations that needs to be solved simultaneously to obtain a solution or if the function itself is not possible to get on a explicit algebraic state form. The second method solves the equation directly for the algebraic state and is thus used for simple equations where iteration is not needed.

$$z = f(x, u) \quad (2.18)$$

## 2.4 Pressure - flow network model

The idea of block building from Section 2.3 requires a strategic approach for a coupled system like the steam cycle. The steam cycle consists of several liquid holdups, or buffer tanks, that act as capacities and thus smooths the dynamics of the system. There are also several static valves and flow control elements that creates fast dynamics. Therefore, to obtain a system with fast and small dynamic these capacities and flow elements should be alternated. (Mazzi N. and A., 2015, p.544) This technique of alternating capacities and flow elements is called a pressure-flow network model in which divides the system on a grid like manner. (J., 2017) The pressure node consists of two inlet streams, the current and the succeeding mass flow of the node, for which the dynamic mass balance of the corresponding tank is solved by integration. The variables solved in the ODE, such as the liquid holdup, is then used to calculate the inlet pressure as a state, which makes the system stiff. The pressure node is therefore considered a dynamic block element. The inlet and the outlet pressure is used to calculate the outlet mass flow through the flow element. The flow element uses the valve equation and is thus considered a static block element.

An example model of the pressure-flow network model is represented in Figure 2.3.

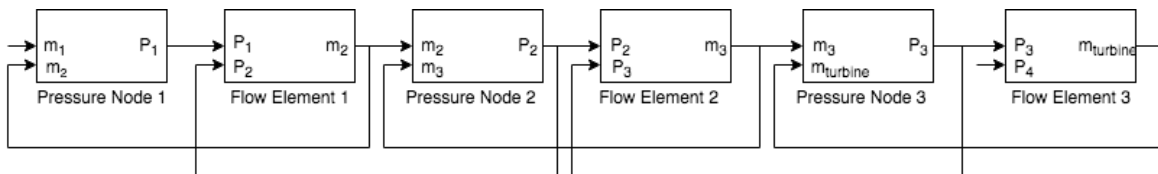


**Figure 2.3:** Pressure Nodes and Flow Elements for the open steam cycle

## 2.5 PID control

The aim of adding control in process control is for the controller to counteract a disturbance, DV, in the system. For a basic feedback controller this is done by measuring the output of the controlled variable, CV, and adjusting the manipulated variable, MV, until the CV has reached its desired setpoint. (S. and C. (2012)) The first step in the design of a control system is to categorize the inputs, MV's and DV's, and the outputs, CV's of the system. A flow sheet is made on the base of these variables and a control structure, such as feedback, is chosen. A widely used feedback controller is the PID-controller, which is built on three terms, Proportional(P)-, Integral(I)- and Derivative(D) control, which are related through Equation 2.19 for the Parallel (ideal) form. The corresponding transfer function is shown in Equation 2.20.

$$u(t) = u_0 + K_c \left[ e(t) + \frac{1}{\tau_I} \int_0^t e(t) dt + \tau_D \frac{de(t)}{dt} \right] \quad (2.19)$$

$$\frac{U(s)}{E(s)} = K_c \left[ 1 + \frac{1}{\tau_I s} + \tau_D s \right] \quad (2.20)$$

where  $e(s)$  is the error in the measured output,  $y$ , from its desired setpoint,  $y_s$ .

### 2.5.1 SIMC - tuning

To ensure proper tuning of a PID-controller a systematic approach is recommended. There are several ways to tune a PID-controller, such as the Ziegler and Nichols IMC PID-tuning and the SIMC tuning method. As the IMC tunings are found to give aggressive response for non-integrating responses, the proposed SIMC (Skogestad-Internal-Model-Control) tunings will be used in this project. (S., 2003) (Skogestad, 2004)

The tuning procedure is divided into two main steps.

The first step consists of obtaining the first- or second- order plus delay model from the step response on the form shown in Equation 2.21. (S., 2003)

$$g(s) = \frac{k}{(\tau_1 s + 1)(\tau_2 s + 1)} e^{-\theta s} \quad (2.21)$$

for large  $\tau_1$  ( $>80$ ) the process is not expected to reach a steady state within a reasonable time period and can be approximated as an integrating process as shown in Equation 2.22. Example plots of an steady state and integrating step response are demonstrated in Figure 2.4 and 2.5, respectively.

$$g(s) = \frac{k}{(\tau_1 s + 1)} e^{-\theta s} \quad (2.22)$$

$$g(s) \approx \frac{k}{\tau_1 s} e^{-\theta s} \quad (2.23)$$

$$g(s) = \frac{k'}{s} e^{-\theta s} \quad (2.24)$$

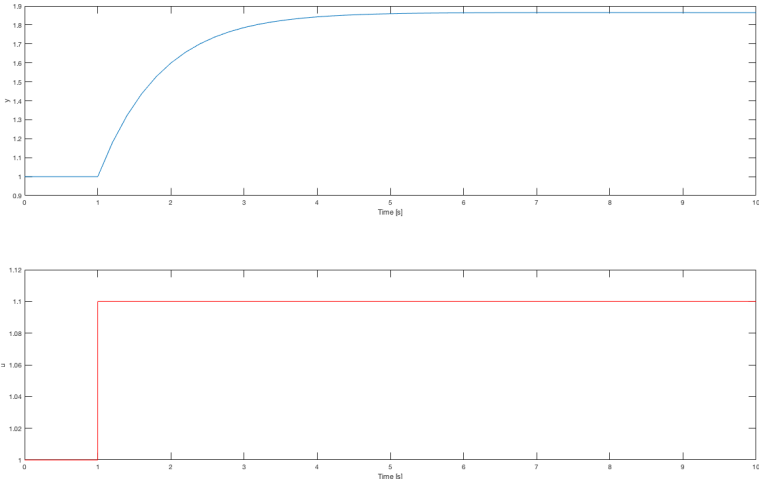


**Figure 2.4:** Example plot of a steady state step response

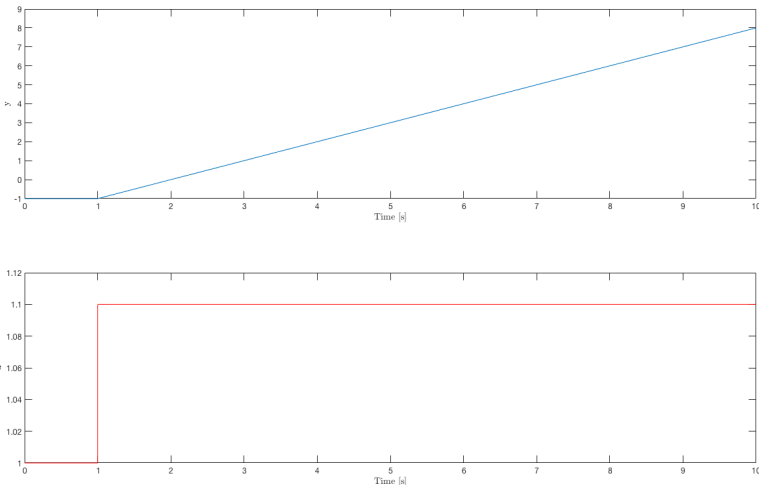


**Figure 2.5:** Example plot of an integrating step response

The second step is to derive the controller settings. The following parameters are noted and the controller tunings derived in Table 2.2.

- $k$ , process gain  $\frac{\Delta y(\infty)}{\Delta u}$
- $k'$ , integrating process gain  $\frac{k}{\Delta t}$
- $\theta$ , Effective time delay
- $\tau_1$ , Dominant lag time constant
- $\tau_2$ , Second-order lag time constant
- $\tau_c$ , closed loop time constant

A P-controller only requires the controller gain,  $K_c$ , and can compensate for the disturbances, but it cannot eliminate the offset completely. If it is desired to keep the controlled variable at its setpoint, a PI- or PID-controller is recommended. PI-settings require the controller gain  $K_c$  and the integral time constant  $\tau_I$ , whereas a second order response in the output will require a PID-controller that includes the derivative time constant,  $\tau_D$ . (S., 2003)

Process	$K_c$	$\tau_I$	$\tau_D$
Integrating	$\frac{1}{k'} \frac{1}{\tau_c + \theta}$	$4(\tau_c + \theta)$	$\tau_2$
Steady state	$\frac{1}{k} \frac{\tau_1}{\tau_c + \theta}$	$\min\{\tau_1, 4(\tau_c + \theta)\}$	$\tau_2$

**Table 2.2:** SIMC controller tunings for PID-control



## 3 — Modelling of the steam cycle

In this chapter the process of modelling a steam cycle is presented. The initial model was inspired from a basic steam cycle MATLAB script by my supervisor, Sigurd Skogestad, and further adjusted and advanced throughout the project. Parts of this steam cycle model was also inspired from (Skogestad, 2009).

### 3.1 Assumptions

Through Section 2.2, assumptions were made in the governing equations for the dynamic states. These assumptions were made to simplify the equations of the steam cycle. Among these there were also made other assumptions through out the modelling, represented in the list below. It is important to clarify that the process modelled in this project is the open steam cycle in which the split from the flow out of the pump into the boiler inlet steam and the bypass stream is not active.

- The process that is modelled is the open steam cycle
- The steam cycle is a pure power generating process
- No chemical reactions
- Steam and flue gas is assumed ideal gases
- Constant heat capacities
- No radiation
- Constant heat transfer coefficient, UA
- Arithmetic mean was used to approximate the temperature difference over the heat exchangers
- Known inlet temperature,  $T_0$  and  $T_{G0}$  for the steam and flue gas respectively in the open steam cycle equal to 45 °C and 1000 °C, respectively.
- Reference temperature in the enthalpy calculation is set to be  $T_{ref} = 45$  °C

- The boiling temperature of water is assumed to be 45 °C at  $P = 0.096$  Bar
- Saturated steam in the boiler
- All of the inlet flow into the boiler is assumed to be in liquid phase
- The steam out of the turbine is assumed to be in gas phase
- Constant initial pressure  $P_0 = 130$  Bar
- Constant pressure out of the turbine  $P_4 = 0.096$ Bar
- Known flue gas flow,  $\dot{m}_G$  and  $\dot{m}_{G2}$  for the heat exchangers to  $7 \text{ kg s}^{-1}$
- The linear valve equation is used for calculation of the flows  $\dot{m}_2$ ,  $\dot{m}_3$  and  $\dot{m}_4$
- The Antoine equation was used to compute the saturation pressure out of the boiler,  $P_1$

## 3.2 Model representation

The modelled steam cycle is represented in Figure 3.1.

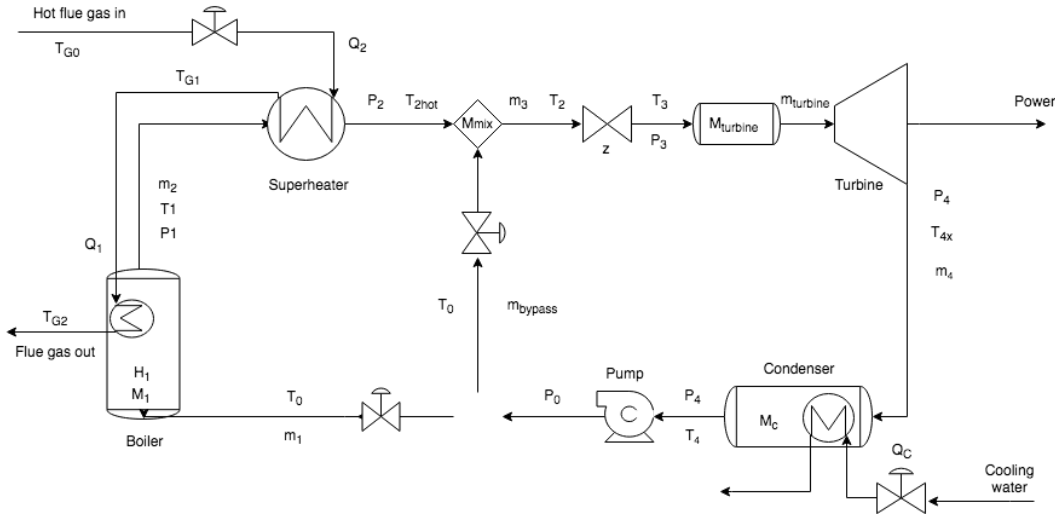


**Figure 3.1:** Process flow diagram for the steam cycle

In the model, water,  $\dot{m}_1$  is fed to the boiler and heated to  $T_1$  by the heat exchanger. The saturated steam,  $\dot{m}_2$ , is additionally heated through the superheater to  $T_{2hot}$ . The superheated steam is mixed with the cooling bypass steam,  $\dot{m}_{bypass}$  by an attenuator until it reaches the desired temperature  $T_2$ . The mixed steam,  $\dot{m}_3$  passes through a valve and a liquid holdup  $M_{turbine}$  for smoother dynamics before the steam,  $\dot{m}_{turbine}$ , is expanded through the power generating turbine. The low pressure steam,  $\dot{m}_4$  is

condensed to  $T_0$  through a cooler. The pressure of the liquid water is increased through a pump before it is sent back through the cycle.

A figure of the turbine subsystem is shown in Figure 3.2.

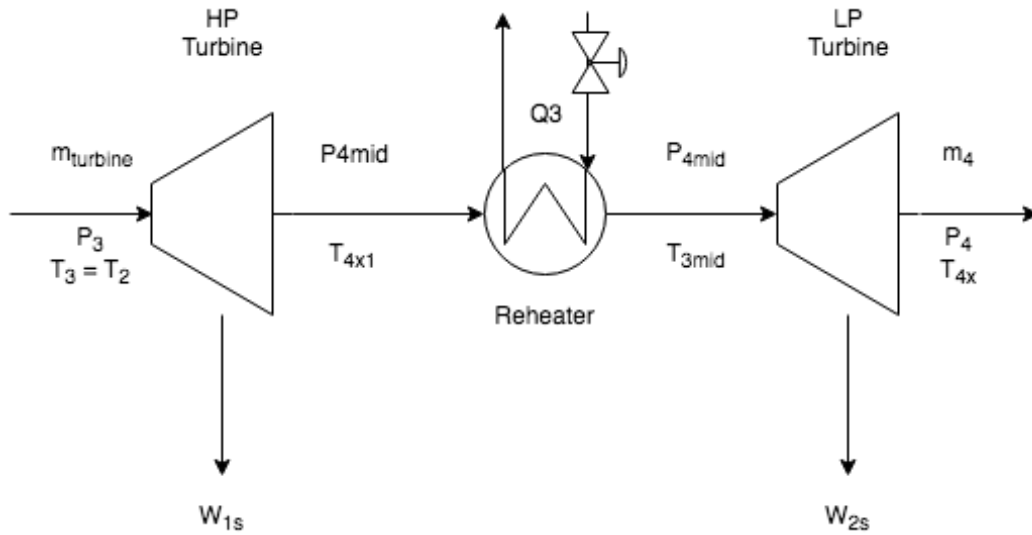


**Figure 3.2:** Process flow diagram for the modeled turbine subsystem

The steam is expanded in two stages by a high pressure and a low pressure turbine. The steam is reheated between the two stages by a heat exchanger (reheater) to  $T_{3mid}$ .

### 3.3 States

The states for the steam cycle process is listed in Table 3.1 below and separated into two categories: dynamic and static states. Dynamic states are determined from the integration of the state on its differential from the assumption of a change in the behaviour of the state with respect to time. The static states are solved from algebraic equations and assumed to be in steady state.

Subsystem	Dynamic states	Static states
Boiler	$M_1, H_1$	$T_1, T_{G2}, P_1$
Superheater		$T_{2hot}, T_{G1}$
attemperor	$M_{mix}, T_2$	$P_2$
Turbine	$M_{turbine}, P_3$	$P_{4mid}, T_{4x1}, T_{4x}, W_{s1}, W_{s2}$
Reheater		$T_{G3}, T_{3mid}$
Condenser	$M_c, T_4$	

**Table 3.1:** The dynamic and static states organized for which subsystem they are calculated from

The units used for the states were used on SI format and are found in Table A.1 in Appendix A.1.

### 3.4 Steam cycle power plant

The subsystems of the steam cycle simulation are constructed with the pressure-flow network model described in Section 2.4. The liquid holdup in the boiler, attemperor, turbine and condenser act as buffer capacities, storing mass, which is modelled through dynamic mass balances. These capacities are alternated with the respected flow elements such as the superheater, HP turbine inlet valve, reheater and the pump which is used for flow control.

#### 3.4.1 Boiler

The first stage of modelling the open steam cycle started with the boiler. The dynamic mass conservation and energy conservation is maintained by modelling the liquid hold up,  $M_1$ , and enthalpy of the steam out of the boiler,  $H_1$ , as a set of ODEs as shown in Equation 3.1 and 3.2 respectively. The derivation can be found in Section 2.2.

$$\frac{dM_1}{dt} = \dot{m}_1 - \dot{m}_2 \quad (3.1)$$

where  $\dot{m}_1$  is considered an input and  $\dot{m}_2$  is computed through the linear valve equation.

$$\frac{dH_1}{dt} = \frac{1}{M_1}(Q_1 + \dot{m}_1 h_0 - \dot{m}_2 h_1) \quad (3.2)$$

A static algebraic equation (AE) is used to calculate the temperature of the steam out,  $T_1$ , as shown in Equation 3.3.

$$0 = H_1 - M_1 h_1 \quad (3.3)$$

where  $h_1$  is the specific enthalpy of the steam out of the boiler represented in Equation 3.4.

$$h_1 = \Delta_{\text{vap}} H^{45^\circ\text{C}} + C_{p,\text{gas}}(T_1 - T_0) \quad (3.4)$$

The set of ODEs and AE form a DAE system on the form mentioned in Section 2.3.1, which is solved separately by the use of an integrator for the dynamic states and a solver block for the algebraic states. The states are looped back to the function block until a converged solution occurs.

### 3.4.2 Superheater

In the superheater there is assumed no holdup and the process is modelled as a straight heat transfer through an algebraic heat balance represented in Equation 3.5

$$0 = Q_2 + h_1 - h_2 \quad (3.5)$$

where  $h_2$  is calculated as shown in Equation 3.6.

$$h_2 = \dot{m}_2(\Delta H_{\text{vap}}^{45^\circ\text{C}} + C_{p,\text{gas}}(T_{2\text{hot}} - T_0)) \quad (3.6)$$

### 3.4.3 Heat exchangers

In the boiler and the superheater, the heat supplied to the water,  $Q_1$  and  $Q_2$ , is done through a collected heat exchanger. It begins by sending through hot flue (methane) gas at 1000 °C through the superheater and continues through the boiler. The values for the heat transfer coefficient multiplied with the area (UA) was obtained from solving Equation 3.7 with steady state data.

The equations for the heat transfer from the flue gas was implemented as AEs in the respected MATLAB functions of the superheater and boiler as described in Section 2.3.3.

$$0 = Q_1 - \dot{m}_G C_{pgG} (T_{G1} - T_{G2}) \quad (3.7)$$

$$0 = \dot{m}_G C_{pgG} (T_{G1} - T_{G2}) - UA_1 \left( \frac{T_{G1} + T_{G2}}{2} - T_1 \right) \quad (3.8)$$

$$0 = Q_2 - \dot{m}_G C_{pgG} (T_{G0} - T_{G1}) \quad (3.9)$$

$$0 = \dot{m}_G C_{pgG} (T_{G0} - T_{G1}) - UA_2 \left( \frac{T_{G0} + T_{G1}}{2} - \frac{T_1 + T_{2,hot}}{2} \right) \quad (3.10)$$

### 3.4.4 Attemperator

The attemperator was modelled as a set of ODEs similarly as presented in Section 2.3.2 formed by the mass and energy conservation on its temperature form, derived in Section 2.2.

$$\frac{dM_{mix}}{dt} = \dot{m}_2 + \dot{m}_{bypass} - m_3 \quad (3.11)$$

$$\frac{dT_2}{dt} = \frac{1}{M_{mix}} \left( \dot{m}_2 (T_{2hot} - T_2) + \dot{m}_{bypass} \left( T_0 - \frac{\Delta H_{vap}}{C_{pg}} - T_2 \right) \right) \quad (3.12)$$

### 3.4.5 Turbine

The turbine subsystem consists of the valve, a liquid holdup ( $M_{turbine}$ ), a high pressure turbine, a reheater and a low pressure turbine. Initially the turbine subsystem was modelled with just one simple high pressure turbine, but because of the large pressure difference it was difficult to obtain a high enough temperature at the outlet and thus risking condensation in the turbine. By introducing a secondary turbine with heating of the steam in between (reheater), the risk of condensation within the turbine can become reduced as well as increasing the total power output as explained in Section 2.1.2. A representation of the process flow diagram for the turbine subsystem is shown in Figure 3.2.

The flow of steam into and through the turbine was modelled with three equations: two static algebraic equations and one dynamic mass balance. This was done by the pressure-flow network principle as mentioned in Section 2.4.

Before the turbine itself a liquid holdup,  $M_{turbine}$  is added to make the dynamics smoother. The dynamic mass balance for the liquid holdup is described in Equation 3.13.

$$\frac{dM_{turbine}}{dt} = \dot{m}_3 - \dot{m}_{turbine} \quad (3.13)$$

The static equations consisted of the valve equation for the flow through the valve,  $\dot{m}_3$  into the liquid holdup and two different approximations from Section 2.1.2 for the flow,  $\dot{m}_{turbine}$  through the turbines.

### Constant volumetric flow

As the flow into the turbine can have a large effect in the power generated two different approximations to compute  $\dot{m}_{turbine}$  were implemented. The first method was assuming constant volumetric flow through the turbine described in Equation 2.3 in Section 2.1.2. The volumetric flow coefficient was computed from nominal values of  $P_3$ ,  $T_3$  and  $\dot{m}_{turbine}$  through the ideal gas law.

### Stodola approximation

The second method used the Stodola Equation to approximate  $\dot{m}_{turbine}$  described in Equation 2.4 in Section 2.1.2. In comparison to the constant volumetric flow approximation the Stodola Equation consists of the added input  $P_4$  which can account for varying pressure drops through the turbine. The Stodola coefficient was computed by Equation 2.5 with nominal values for  $P_3$ ,  $T_3$  and  $\dot{m}_{turbine}$  and a constant value for  $P_4$ .

### Power output and intermediate states

The power produced as well as the intermediate pressures and temperatures were computed by the means of direct static AEs explained in Section 2.3.3. The equation system for the HP and LP turbine is shown in Equation 3.14 and 3.15 respectively.

$$\begin{aligned} P_{4mid} &= P_3 \left( \frac{T_4}{T_3} \right)^{\frac{C_{pg}}{R}} \\ T_{4x1} &= T_3 \left( \frac{P_{4mid}}{P_3} \right)^{\frac{R}{C_{pg}}} \\ W_{s1} &= \dot{m}_{turbine} C_{pg} (T_{4x1} - T_3) \end{aligned} \quad (3.14)$$

$$\begin{aligned}
 T_{4x} &= T_{3mid} \left( \frac{P_4}{P_{4mid}} \right)^{\frac{R}{C_{pg}}} \\
 W_{s2} &= \dot{m}_{turbine} C_{pg} (T_{4x} - T_{3mid});
 \end{aligned}
 \tag{3.15}$$

## Reheater

The reheater between the HP and LP turbine was modelled similarly to the heat exchangers through the Boiler and Superheater as a set of AEs represented in Equation 3.16. The heat transfer coefficient,  $UA_3$ , was found by solving Equation 3.16 with steady state data.

$$\begin{aligned}
 0 &= h_{4mid} - h_{3mid} + Q_3 \\
 0 &= \dot{m}_{G2} C_{pgG} (T_{G0} - T_{G3}) - UA_3 \left( \frac{T_{G0} + T_{G3}}{2} - \frac{T_{4x1} + T_{3mid}}{2} \right) \\
 0 &= Q_3 - \dot{m}_{G2} C_{pgG} (T_{G0} - T_{G3})
 \end{aligned}
 \tag{3.16}$$

where the enthalpies were calculated as shown in Equation 3.17.

$$\begin{aligned}
 h_{4mid} &= \dot{m}_{turbine} (C_{pg} (T_{4x1} - T_0) + \Delta_{vap} H) \\
 h_{3mid} &= \dot{m}_{turbine} (C_{pg} (T_{3mid} - T_0) + \Delta_{vap} H)
 \end{aligned}
 \tag{3.17}$$

### 3.4.6 Condenser

The condenser includes a liquid hold up and is modelled by a set of ODEs. The holdup,  $M_c$ , is computed through the dynamic mass balance and the temperature out of the condenser by solving the dynamic energy balance on its temperature form as represented in Equation 3.18 and 3.19 respectively.

$$\frac{dM_c}{dt} = \dot{m}_{turbine} - \dot{m}_4
 \tag{3.18}$$

$$\frac{dT_4}{dt} = \frac{1}{M_c} \left( \dot{m}_{turbine} (T_{4x} - T_4) + \frac{\Delta H_{vap}}{C_{p,g,steam}} \right) + \frac{Q_c}{C_{p,g,steam}}
 \tag{3.19}$$

### 3.4.7 Pump and valves

The mass flows through the valves and the pump,  $\dot{m}_2$ ,  $\dot{m}_3$  and  $\dot{m}_4$ , were modelled by the use of the linear valve equation as represented in Equation 3.20

$$\dot{m}_i = K_{v,i}z(P_i - P_{i+1}) \quad (3.20)$$

The valve coefficient,  $K_{v,i}$ , is determined from the steady state values for the mass flow and the respected in and outlet pressures and can be found in section A.2

The pressures and mass flows were alternated with dynamic pressure nodes on the pressure-flow network form discussed in Section 2.4 to obtain a system with fast and small dynamics.

## 3.5 Control structure

In this section the possible manipulated, disturbance and control variables are identified as well as a proposed control structure. The PID - controllers are tuned using the SIMC tuning rules from section 2.5.1.

### 3.5.1 MVs, CVs and DVs

Inputs that can be manipulated are called manipulated variables (MVs) and can be paired with states that we wish to keep at given specification, controlled variables (CVs). An input that creates a disturbance in the system is called a disturbance variable (DVs). The identified MV's, CVs and DV's for the steam cycle are listed below.

MVs

- $\dot{m}_1$  - Mass flow at the boiler inlet
- $\dot{m}_{bypass}$  - Mass flow of the bypass stream
- $z$  - Valve at turbine inlet
- $\dot{m}_G$  - Mass flow of the flue gas in the HEX through the boiler and the superheater
- $\dot{m}_{G2}$  - Mass flow of the flue gas in the HEX through the reheater
- $Q_c$  - Heat flow in the condenser

DVs

- $T_0$  - Temperature at the inlet of the boiler and in the bypass stream
- $T_{G0}$  - Inlet temperature of the flue gas
- $\dot{m}_2$  - Mass flow of the steam after the superheater
- $\dot{m}_3$  - Mass flow of the steam after the attemperator
- $\dot{m}_{turbine}$  - Mass flow of steam through the turbine
- $Q_1$  - Heat transfer from the flue gas to the water in the boiler
- $Q_2$  - Heat transfer from the flue gas to the steam in the superheater
- $Q_3$  - Heat transfer from the HEX to the steam at the reheater

Possible CVs

- $M_1$  - Liquid holdup in the boiler
- $T_1$  - Temperature out of the boiler

- $P_1$  - Saturation pressure out of the boiler
- $T_{G1}$  - Temperature in the flue gas out of the HEX through the superheater
- $T_{G2}$  - Temperature in the flue gas out of the HEX through the boiler
- $P_2$  - Pressure in the steam after the superheater
- $T_{2hot}$  - Temperature of the steam after the superheater
- $M_{mix}$  - Holdup of water in the attemperator
- $T_2$  - Temperature of the steam after the attemperator
- $T_3$  - Temperature of the steam at the turbine inlet
- $P_3$  - Pressure of the steam at the turbine inlet
- $M_{turbine}$  - Holdup of steam before the turbine
- $P_{4mid}$  - Pressure after the HP turbine
- $T_{4x1}$  - Temperature after the HP turbine
- $T_{G3}$  - Temperature of the flue gas after the HEX at the reheater
- $T_{3mid}$  - Temperature at the inlet of the LP turbine
- $T_{4x}$  - Temperature after the LP turbine
- $W_{s1}$  - Power output from the HP turbine
- $W_{s2}$  - Power output from the LP turbine
- $T_4$  - Temperature after the condenser

### 3.5.2 Proposed control pairings

A degree of freedom is a variable that is free to be manipulated(MV). From the listed MVs and CVs in the Section 3.5.1 there can be identified 6 degrees of freedom. These MVs can be coupled with the CVs that it is desired regulate.

First the CV's necessary for stable operation such as the liquid holdup  $M_1$  was paired with  $\dot{m}_1$  with a level controller by the "pair-close"-rule as to minimize the effective time delay. (Minasidis V. and N. (2015))

The temperatures in the steam cycle is also relatively important to regulate. Too high temperatures at the turbine inlet will damage the turbine and too low temperatures can lead to condensation and low power output as mentioned in Section 2.1.3 and 2.1.2.

Applying the "pair-close" rule lead to the temperature controllers for the temperature at the HP turbine inlet,  $T_2$  and LP turbine inlet were controlled by manipulation of the bypass flow,  $\dot{m}_{bypass}$  and the flue gas flow at the reheater  $\dot{m}_{G2}$  respectively. Another valuable temperature in the steam cycle is the temperature out of the condenser,  $T_4$ , which is desired to be kept at the border of the vaporization temperature to minimize the amount of cooling water needed.  $T_4$  is therefore coupled with the heat flow from the cooling water,  $Q_c$ .

There are two DOFs left,  $z$  and  $\dot{m}_G$ . As one of the objectives in this project is related to the power output,  $\dot{m}_G$  can be coupled with the total power produced,  $W_{s1} + W_{s2}$ . The latter DOF,  $z$ , can be paired with the saturation pressure at the outlet of the boiler,  $P_1$ , which also can influence the power produced as increased pressure into the turbine directly increases the power production. The input saturation rule is considered in the pairing of  $z$  and  $P_1$  as the saturation pressure is considered a lesser important variable to regulate in this system and can be given up if  $z$  saturates (reaches fully open or fully closed state). (Minasidis V. and N., 2015)

The suggested controller pairings are listed in Table 3.2 and visualized in Figure 3.3 and 3.4.

MV	CV
$\dot{m}_1$	$M_1$
$\dot{m}_{bypass}$	$T_2$
$\dot{m}_{G2}$	$T_{3mid}$
$Q_c$	$T_4$
$\dot{m}_G$	$W_{s1}+W_{s2}$
$z$	$P_1$

**Table 3.2:** Proposed controller pairings for the open steam cycle model

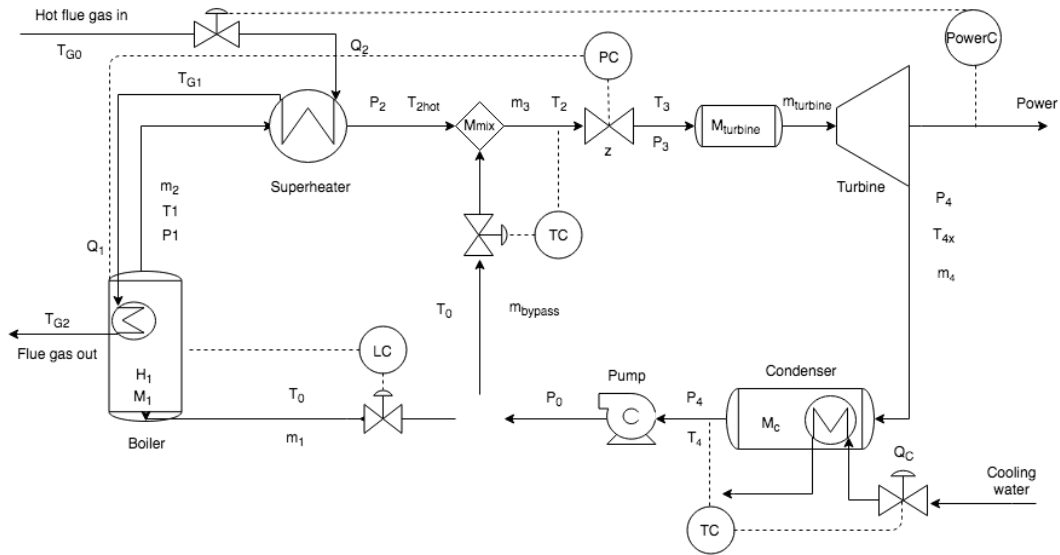


Figure 3.3: Process flow diagram of the steam cycle with the proposed control structure

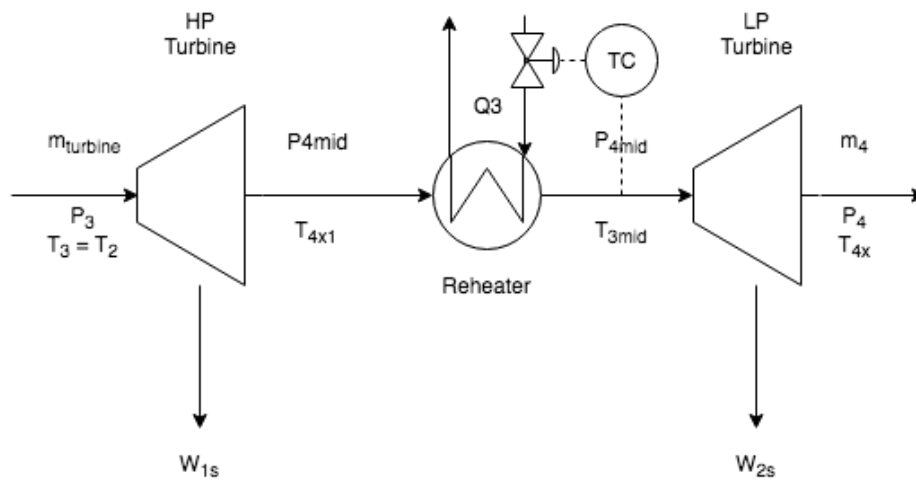
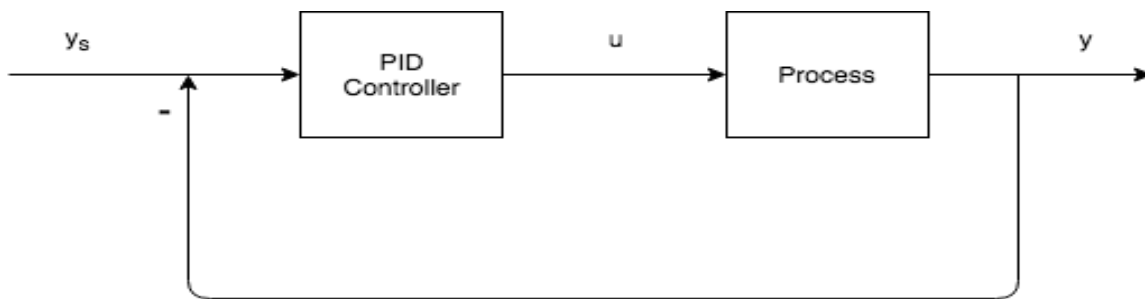


Figure 3.4: Process flow diagram of the turbine subsystem with the proposed control structure

### 3.5.3 Controller tuning

To tune the controllers an open loop step response was made for the selected controller pairings determined in Section 3.5.2. The response of a step in the input (MV) on the output (CV) was determined as integrating for the liquid holdup in the boiler,  $M_1$  and steady state for the latter pairings.

The holdup controller (MC) for the boiler is a P-controller so that it dampens the disturbances in the system; this adds stability to the system. (A. and S., 2003) As explained in Section 2.5.1 a PI-controller would attempt to maintain the holdup to its mass setpoint and thus incoming disturbances would not be dampened. All of the controllers were tuned according to the SIMC-tuning rules as explained in Section 2.5.1 and modelled in Simulink by the use of the PID-controller block in MATLAB. The error between the measured state and the setpoint is multiplied with the PID-control block and added to the nominal value of the manipulated input. An example of the PID-controller modelling is presented in Figure 3.5.



**Figure 3.5:** Example of how to model PID-control in Simulink

## 4 — Simulation

This chapter presents the simulations that were made based on the steam cycle model presented in Chapter 3. The first aim of the project was to create a stable model where step responses could be made to study the effect on outputs such as the power and liquid hold up, both with and without activation of controllers. The initial conditions (design data) was checked and recalculated by hand throughout the project and can be found in Appendix A.3. The constant parameters are listed in Table A.3 in Appendix A.2. The controllers were tuned from open loop step responses and verified through closed loop setpoint changes as plotted in Appendix A.5. The setpoints for the states are listed in Table A.6 in Appendix A.4

### 4.1 Stability of simulation

Plots of the liquid holdup in the boiler, attemperator and before the turbine were made to check if the system is stable without any active controllers.

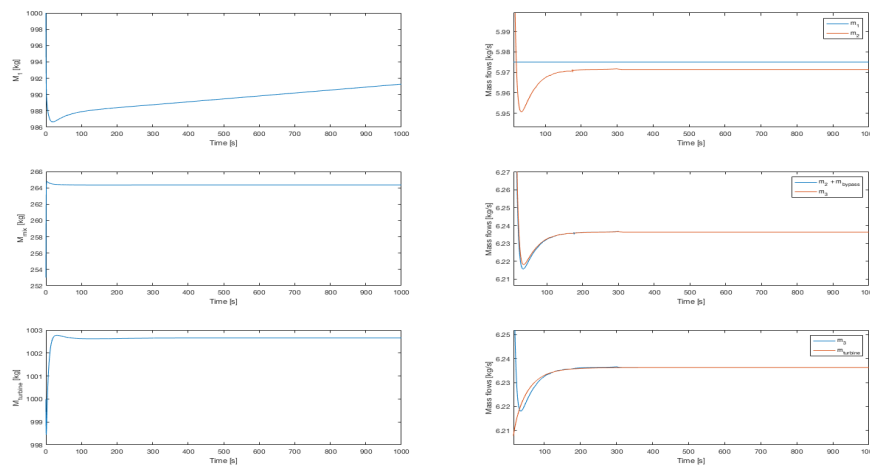


**Figure 4.1:** Plot of the liquid holdups and flows for the boiler, attemperator and turbine at design conditions with no control

## 4.2 Stodola vs Constant volumetric flow

Plots were made of the system with both the Stodola Equation and the Constant volumetric flow approximation of the turbine inlet mass flow,  $m_{turbine}$ , as shown in Figure 4.3 and 4.2, respectively.

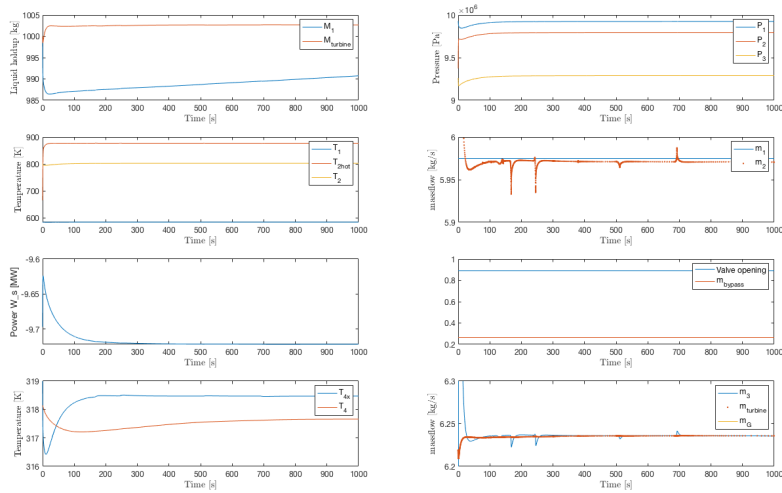


**Figure 4.2:** Plot of the most important variables at steady state using constant volumetric flow

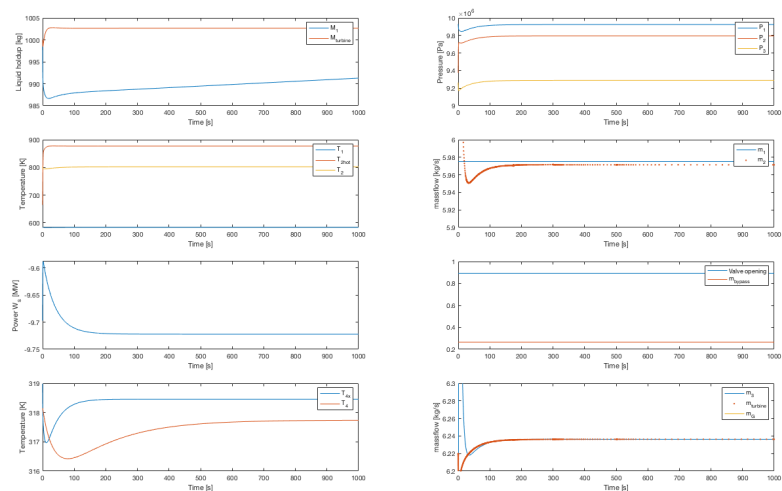


**Figure 4.3:** Plot of the most important variables at steady state using Stodolas Equation

Plots of the two approximation methods with an introduced disturbance in the valve before the turbine,  $z$ , to see how they handled the disturbance are represented in Figure 4.4 and 4.5 for the constant volumetric flow and Stodola approximation of  $\dot{m}_{turbine}$  respectively.

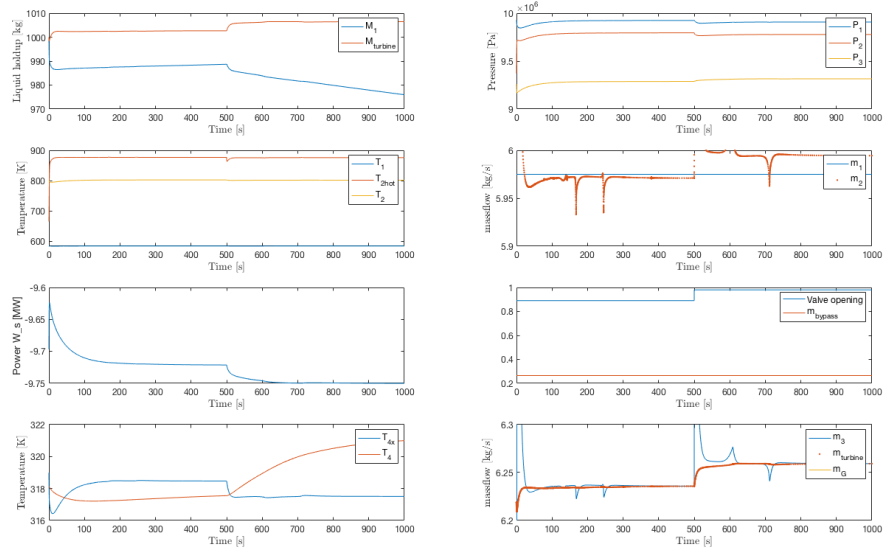


**Figure 4.4:** Plot of a 10% step on  $z$  when using the constant volumetric flow approximation

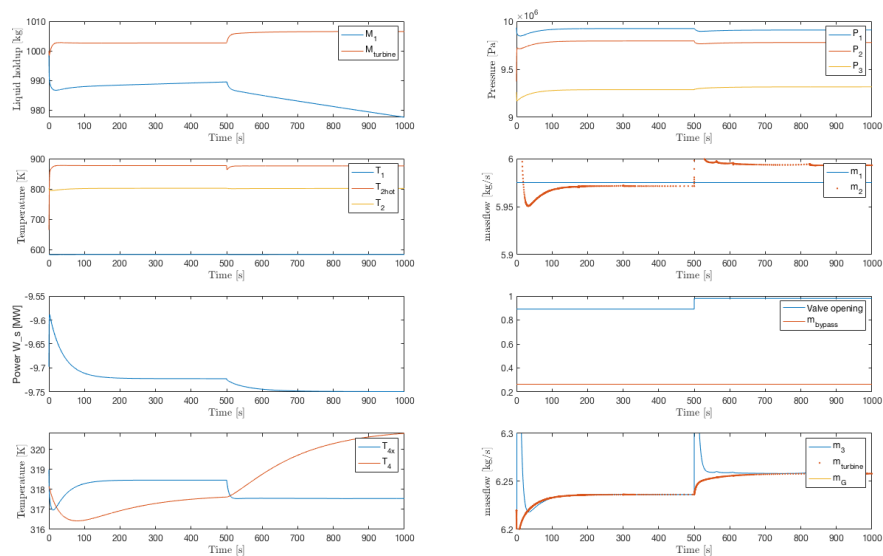


**Figure 4.5:** Plot of a 10% step on  $z$  when using the Stodola equation approximation

### 4.3 Open loop responses without holdup control

The Stodola approximation were used for the latter simulations. Open loop responses without any active controllers for the boiler inlet flow  $\dot{m}_1$ , bypass stream  $\dot{m}_{bypass}$ , valve position  $z$  and flue gas flow  $\dot{m}_G$  were made and are presented in the subsections below. Open loop step responses were also made for the latter inputs which can be found in Appendix A.5.

#### 4.3.1 10% increase in inlet flow, $\dot{m}_1$

A 10% increase was introduced to the inlet flow at  $t = 50$ s of the boiler  $\dot{m}_1$  as shown in Figure 4.6.

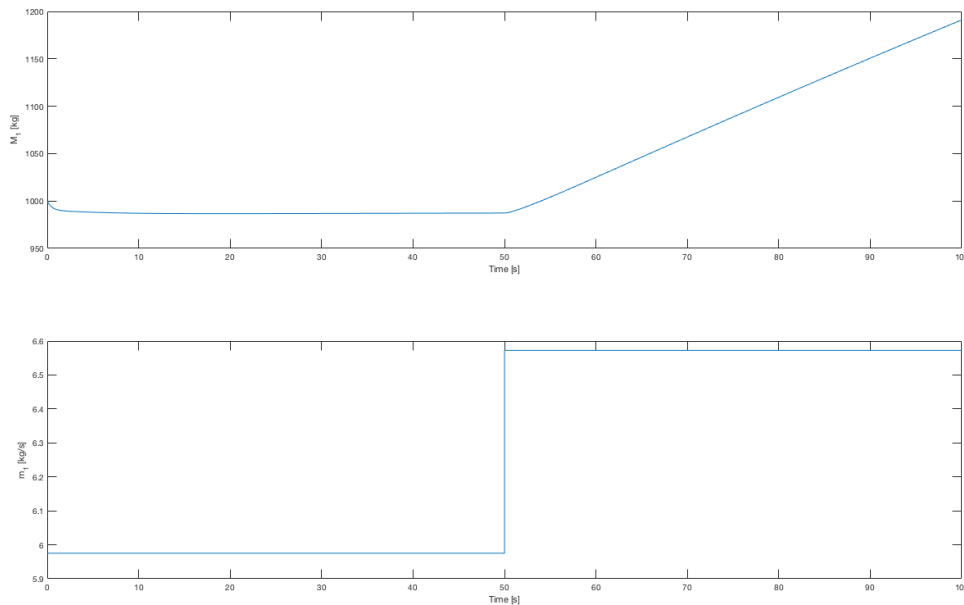


**Figure 4.6:** Plot of the response on  $M_1$  after a 10% step of  $\dot{m}_1$

### 4.3.2 10% increase in bypass flow, $\dot{m}_{bypass}$

A 10% increase was introduced at  $t = 500\text{s}$  in the bypass steam  $\dot{m}_{bypass}$  as shown in Figure 4.7.

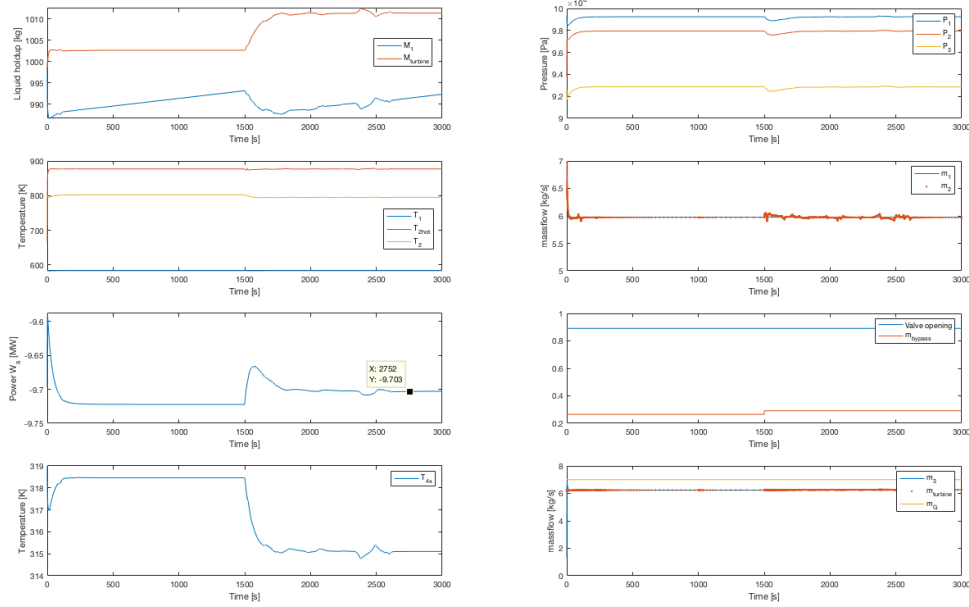
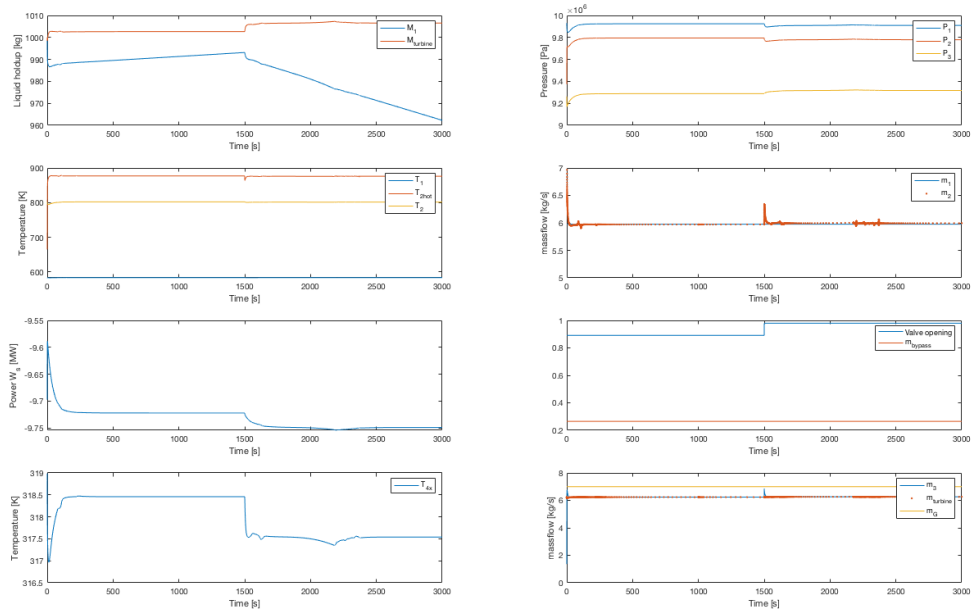


Figure 4.7: Plot of the response after a 10% step of  $\dot{m}_{bypass}$

### 4.3.3 10% increase in valve position, $z$

An 10% increase was introduced at  $t = 1500$ s in the valve position,  $z$ , as shown in Figure 4.8.



**Figure 4.8:** Plot of the response after a 10% step of  $z$

### 4.3.4 Variation of flue gas flow, $\dot{m}_G$ in the heat exchanger

The flow rate of the flue gas in the HEX was varied at  $t = 50\text{s}$  to check for limitations with regards to system instability or unfeasible conditions.

#### 1% increase in flue gas, $\dot{m}_G$

The highest possible increase in flue gas was found to be 1% and limited by convergence of the simulation, represented in Figure 4.9.

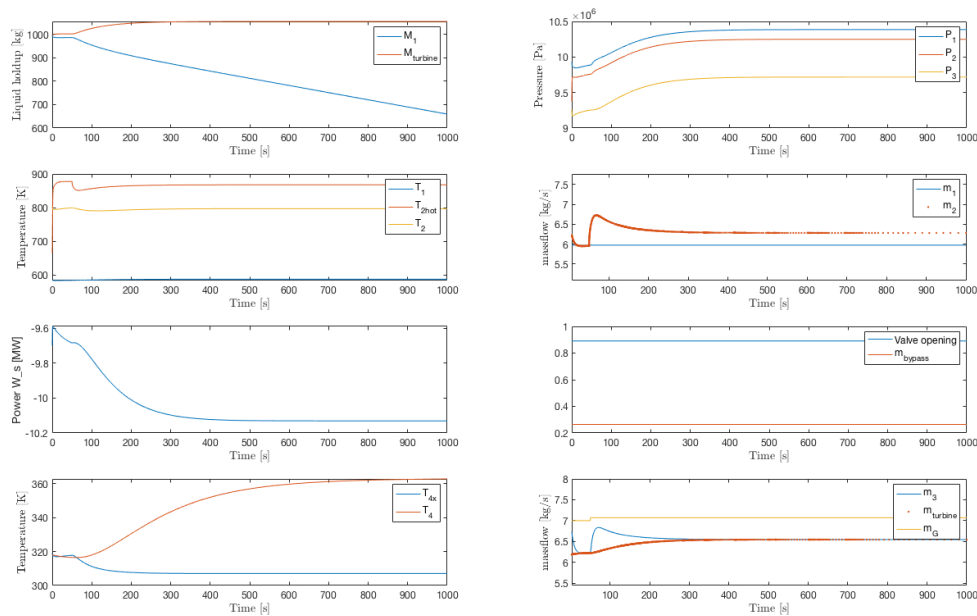


**Figure 4.9:** Plot of the response after a 1% step of  $\dot{m}_G$

#### 10% decrease in flue gas, $\dot{m}_G$

The lowest possible decrease in flue gas was found to be 10% and limited by convergence of the simulation, represented in Figure 4.10.

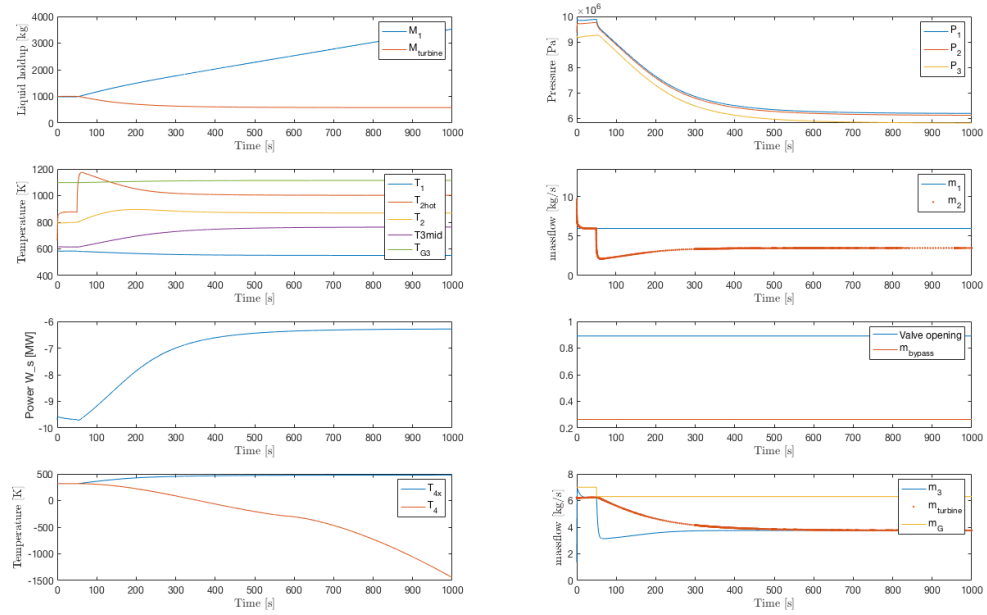


Figure 4.10: Plot of the response after a -10% step of  $m_G$

## 4.4 Step responses with the holdup and temperature controllers active

Despite the fact that the liquid holdup in the boiler revealed to not be completely stable at design conditions it was possible to tune the holdup controller.

The controller gain, integral time  $\tau_I$  and the selected closed loop time constant  $\tau_c$  for the respected controllers are represented in Table 4.1. The corresponding step response plots used in the tunings are found in Appendix A.5. The state setpoints used in the simulation are rendered in Table A.6 in Appendix A.4.

Controller	Response	$K_c$	$\tau_I$	$\tau_c$
MC	Integral	0.1465	-	1
$TC_{T_2}$	Steady state	-0.1082	-	1
$TC_{Reheater}$	Steady state (step)	0.2800	-	$\tau_1 = \text{very small}$
$TC_{Condenser}$	Steady state	1.9843e6	-	1
PC	Steady state with undershoot	-1.7820e-5	3	1
PowerC	Steady state	-2.1620e-7	-	100

**Table 4.1:** Controller tunings for the respected controllers

The control loops for the holdup  $M_1$  controller as well as the temperature controllers for  $T_2$ ,  $T_{3mid}$  and  $T_4$  were closed. Closed loop step responses of the setpoints were introduced for the holdup and temperature  $T_2$  to test the controllers, as well as open loop step responses in  $z$  and  $\dot{m}_G$ . The plots are with intermediate holdup controller,  $K_{c1} = 0.1465$  if not otherwise specified.

### 4.4.1 Closed loop 10% setpoint change $M_{1s}$

A 10% increase was made in the setpoint of  $M_1$  at  $t = 1000s$ .

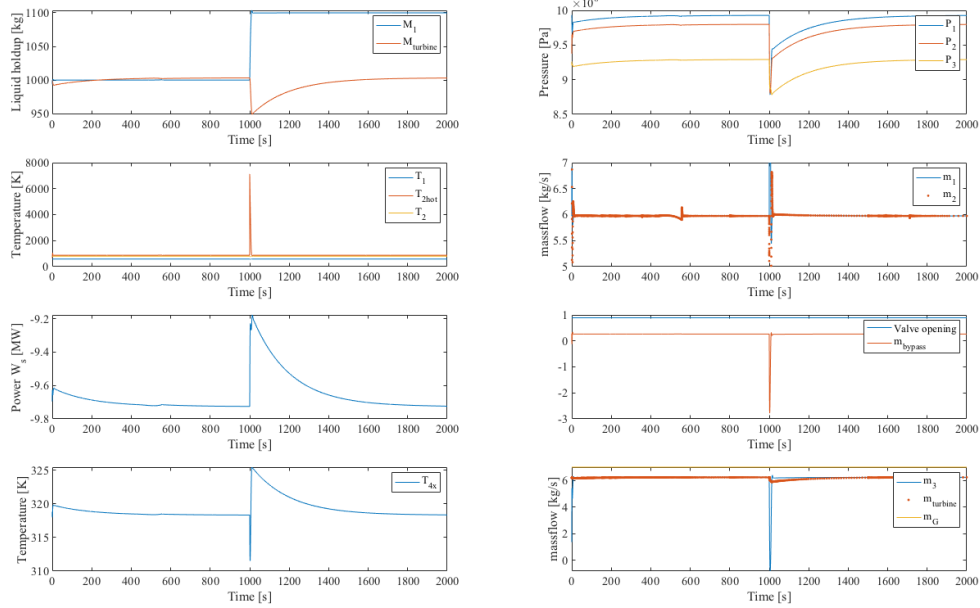


**Figure 4.11:** Plot of the response after a 10% setpoint change of  $M_1$

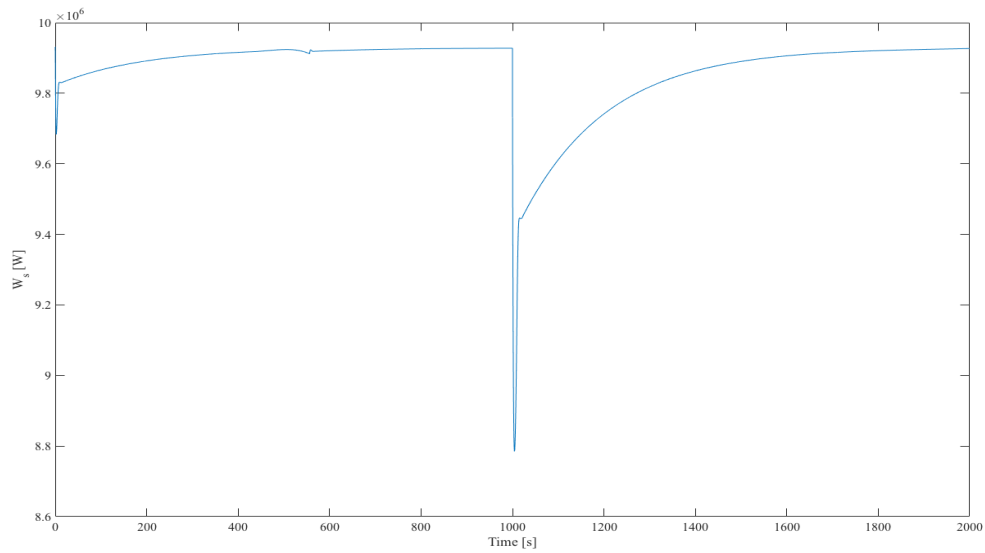


**Figure 4.12:** Plot of the response in  $W_s$  after a 10% setpoint change of  $M_1$

### 4.4.2 Closed loop 10% setpoint change in $T_{2s}$

A 10% setpoint change was made of  $T_2$  at  $t = 1000s$ .

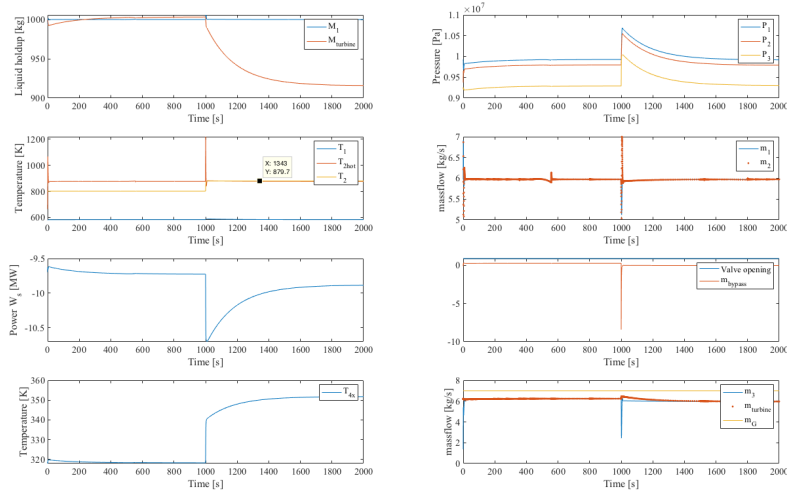


Figure 4.13: Plot of the response after a 10% change in the setpoint of  $T_2$

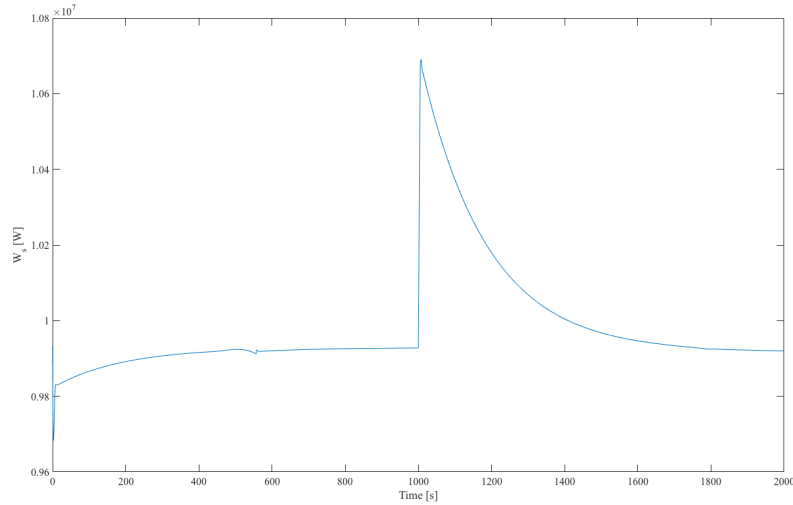
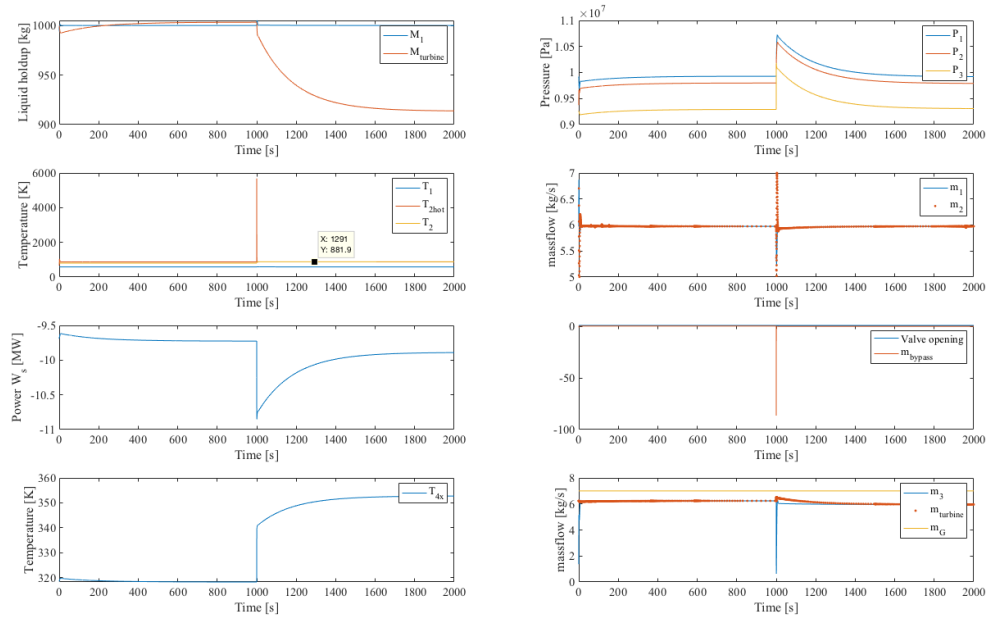
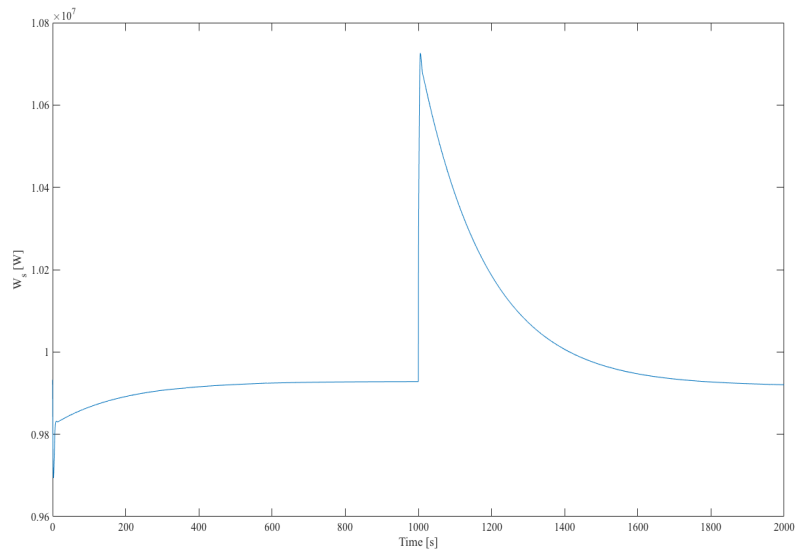


Figure 4.14: Plot of the response in  $W_s$  after a 10% change in the setpoint of  $T_2$

The same step response was repeated with a 10 times larger temperature controller speed,  $K_{\text{bypass}} = -1.0820$ .



**Figure 4.15:** Plot of the response after a 10% change in the setpoint of  $T_2$ .  $K_{bypass} = -1.0820$



**Figure 4.16:** Plot of the response in  $W_s$  after a 10% change in the setpoint of  $T_2$ .  $K_{bypass} = -1.0820$

### 4.4.3 10% step increase in the valve position, $z$

A 10% step increase in  $z$  was introduced at  $t = 1500s$  with fast, intermediate and slow holdup control to see the effect on the power output, represented in Figure 4.17, 4.18 and 4.19 respectively.

Fast controller speed.  $Kc1 = 14.64$

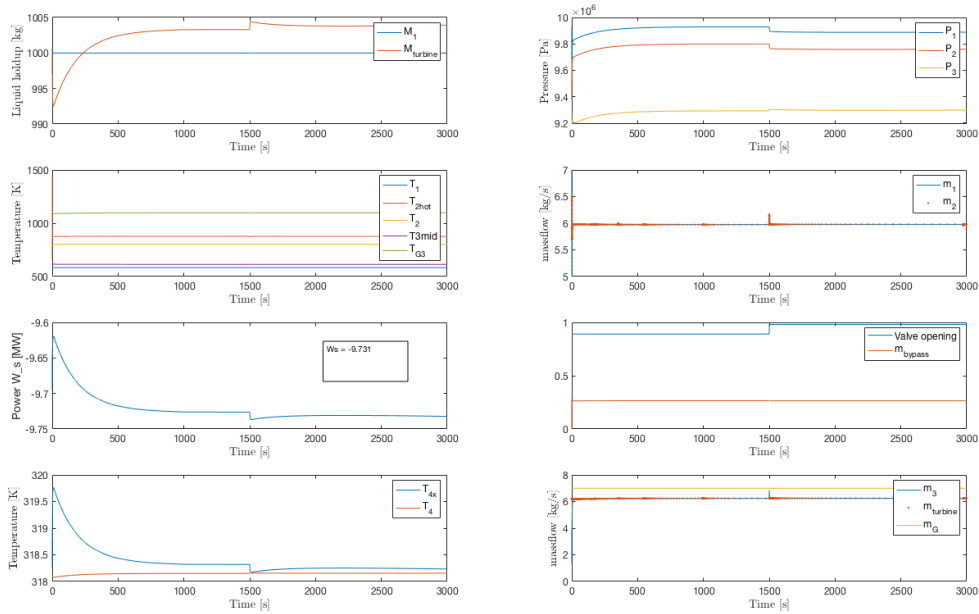


Figure 4.17: Plot of the response after a 10% step of  $z$  with MC and TCs on.  $Kc1 = 14.64$

Intermediate controller gain.  $Kc1 = 0.1464$

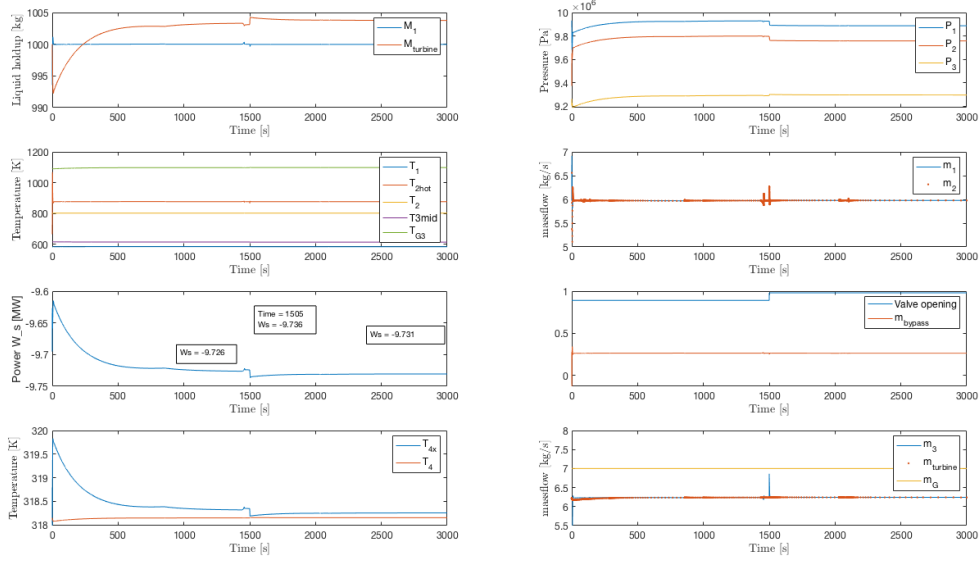


Figure 4.18: Plot of the response after a 10% step of  $z$  with MC and TCs on.  $Kc1 = 0.1464$

Slow controller gain.  $K_{c1} = 0.01464$

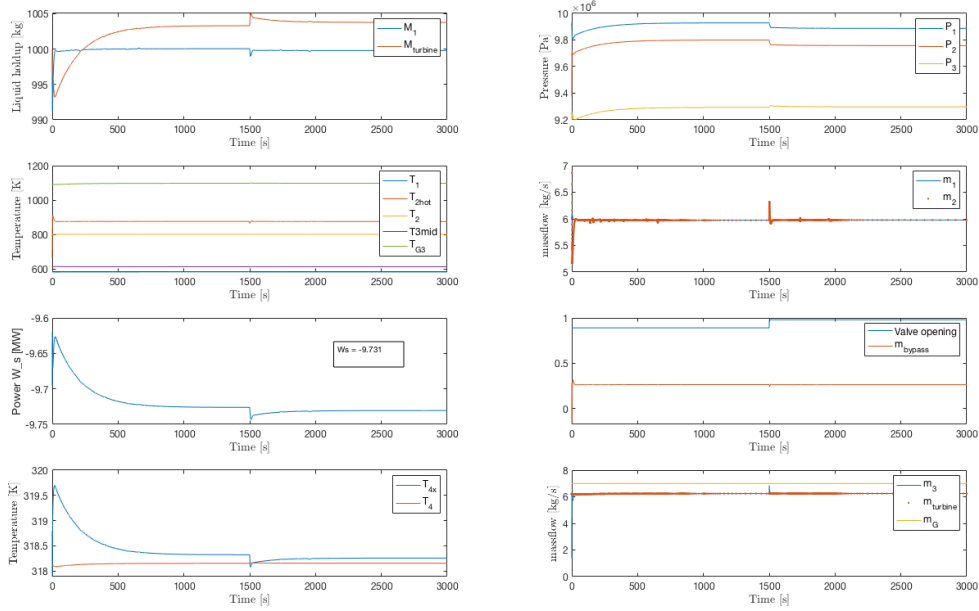


Figure 4.19: Plot of the response after a 10% step of  $z$  with MC and TCs on.  $K_{c1} = 0.01464$

Plots of the power output for all three cases

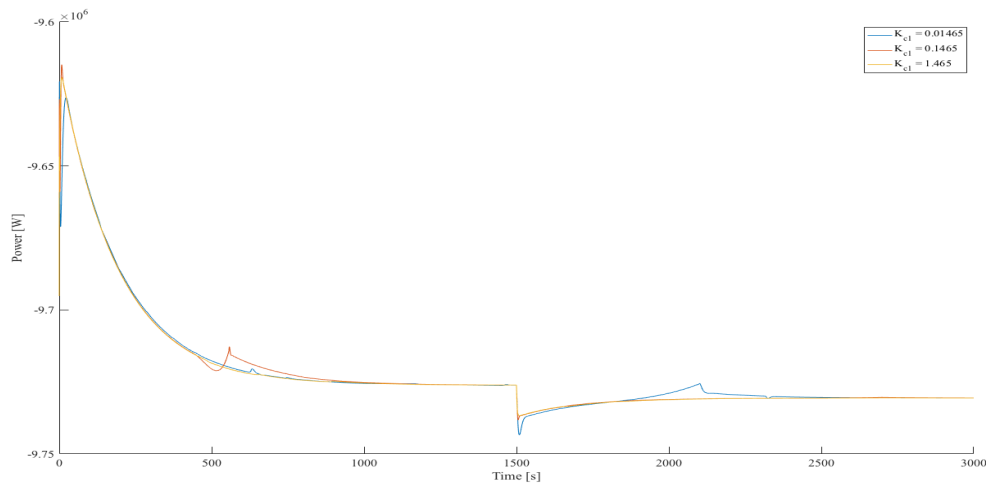


Figure 4.20: Plot of the response after a 10% step of  $z$  with MC and TCs on

### 4.4.4 Variation fo the flue gas flow, $\dot{m}_G$ in the heat exchanger

The flue gas in the heat exchanger was varied at  $t = 1500s$  to check for limitations with regards to stability and feasibility of the system.

1% increase in  $\dot{m}_G$

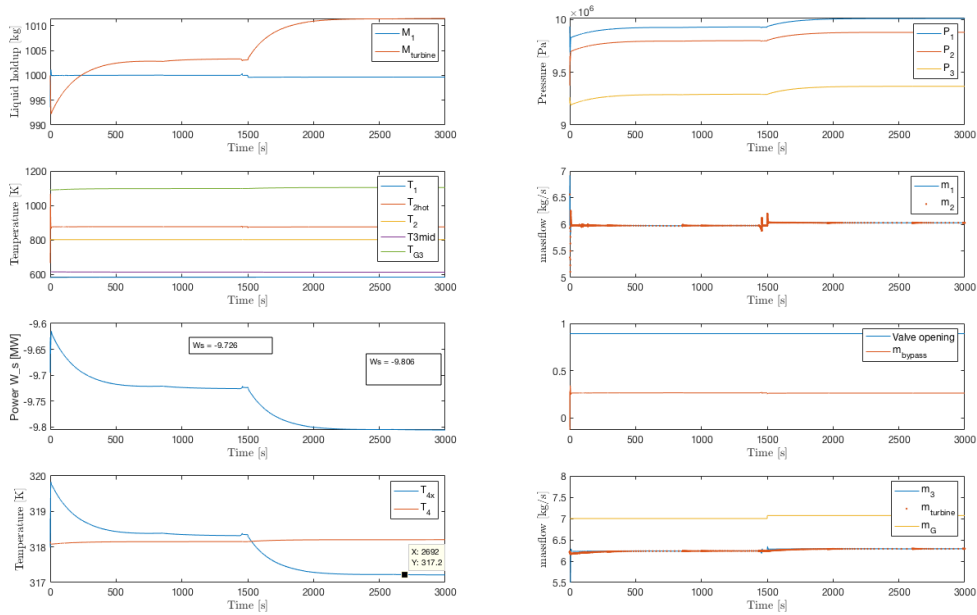
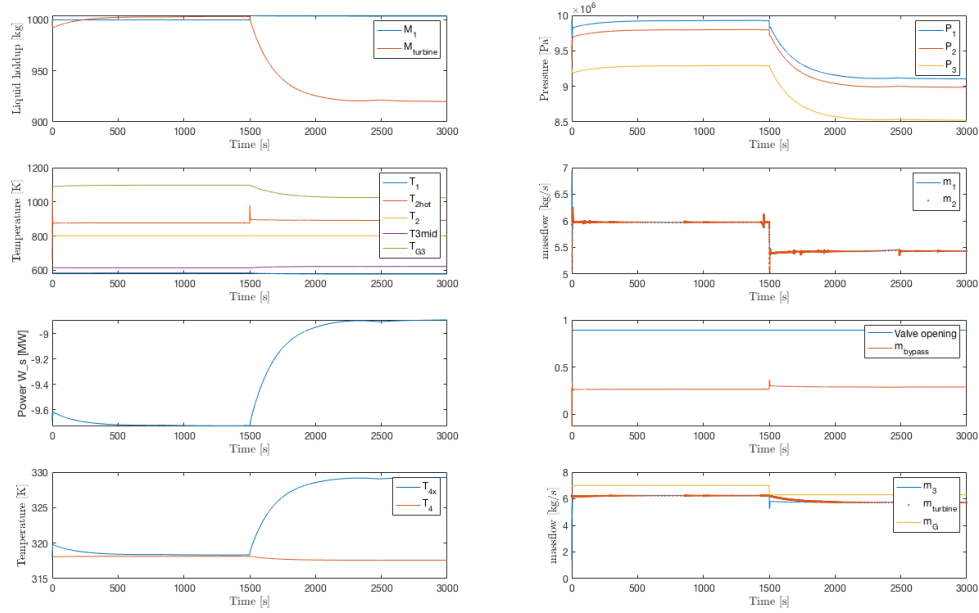


Figure 4.21: Plot of the response after a 1% step of  $\dot{m}_G$  with MC and TCs on.  $Kc1 = 0.1464$

10% decrease in  $\dot{m}_G$



**Figure 4.22:** Plot of the response after a -10% step of  $\dot{m}_G$  with MC and TCs on.  $Kc1 = 0.1464$



## 5 — Discussion and further recommendations

The first objective of this project was to create a stable simulation model of the steam cycle. What was identified in the constructed simulation model was that the level in the boiler had a constant increase as seen from Figure 4.1. At ideal design (initial) conditions this is not supposed to occur as the nominal values for the inlet flow and outlet flow are determined to be equal. This was found to not be the case as the inlet flow is set as a constant input and the outlet flow is calculated through the valve equation. The small deviations in the pressure affects the outlet flow greatly in which causes accumulation or reduction in the liquid holdup. This is consequently an error that can affect the accuracy of the results, especially with regards to the non-controlled step responses from Chapter 4.3.

The use of Stodolas Equation as an approximation of the turbine inlet flow demonstrates a more stable calculation of the flows compared to the constant volumetric flow. The peaks from Figure 4.2 is most likely caused by small pressure variations that propagate through the system. Considering the constant volumetric flow approximation is only recommended for systems during design conditions, it will not account properly for variations in the system and thus the system struggles to converge. (Cooke, 1985) The same is seen for the plots with a 10% step increase in  $z$  in Figure 4.5 and 4.4, where the mass flow,  $\dot{m}_3$ , into the valve causes several peaks when using the constant volumetric flow approximation and struggles to converge towards the computed mass flow into the turbine. These problems also propagate to the mass flow computed out of the boiler and thus represents a strong interconnectedness between the computation of the various mass flows. A recommendation for this problem can be to both model the outlet flow,  $\dot{m}_2$ , with another equation than the linear valve equation and to increase the liquid holdups to slow down the dynamics further.

It was possible to tune the level controller even if the level never reached a proper steady state before the introduced step in  $\dot{m}_1$ . The main reason for this is because the liquid holdup has an integrating response, such that the already existent linear increase is mainly enlarged when introduced to disturbances, as seen in Figure 4.6. The effect of

the holdup controller is verified by the setpoint change of  $M_1$  in Figure 4.11 and 4.12 the liquid holdup stabilizes the system quickly and produces a temporarily increase in the power output.

In the setpoint change of  $T_2$  from Figure 4.13 and 4.14 it can be identified that the controller works and stabilizes the system, but the temperature offset is too large to be accepted as the temperature  $T_2$  increases above the current allowed limit of 630°C, mentioned in Section 2.1.3. In the same setpoint change with a larger controller gain for the temperature controller the offset is reduced to an acceptable value. It is therefore recommended to use a smaller  $\tau_c$  for this controller to obtain reasonable temperature control.

In the step response of the bypass flow in Figure 4.7,  $M_1$  and  $M_{turbine}$  uses a long time to stabilize. This is most likely caused by the slow dynamics within the system as well as the inconsistent mass flow out of the boiler,  $\dot{m}_2$ . The increase in bypass flow causes the temperature and the pressure at the inlet of the turbine to drop and thus less power is produced. The temperature out of the turbine,  $T_{4x}$  drops below the vaporization temperature (318.15K) which in this case, where the outlet pressure of the turbine is assumed constant, would cause condensation through the turbine.

The 10% increase in valve position from Figure 4.8 lead to an increased power output as expected from the increase in  $P_3$ . From the controlled step responses in Figure 4.17, 4.18, 4.19 and 4.20 there was seen little difference in the fast and intermediate level controllers for the power output peak. The reason for this can be the large liquid holdup in  $M_{turbine}$  that causes slow dynamics through the turbine. If a higher sensitivity is desired for the level controller on the produced power output, the holdups before the turbine can be reduced, but then on the cost of stability of the simulation. The slower level controller had a more distinct peak as the disturbance is regulated more slowly, which also lead to the power using longer time to reach steady state. This indicates that it might be possible to use  $M_1$  for energy storage, as the effect is present. It is still recommended to reevaluate this statement when better modelling is made with regards to  $\dot{m}_2$  and the holdup dynamics withing the system.

The limitations with respect to the flue gas was caused by convergence problems as well as low turbine outlet temperature for the increase in  $\dot{m}_G$ . From the non-controlled step response in Figure 4.9 the increase in flue gas is expected to increase the temperature of the steam and lead to an increase in the pressure. The increased pressure causes the turbine to generate more power, which does occur in the plot. The  $M_1$  decreases rapidly as a result of the increased flow out,  $\dot{m}_2$ . The reason for this is because of the increase in pressure that also increases the flow through the valve equation. In the controlled step response of 1% increase in flue gas from Figure 4.21, the decrease in the holdup from the difference in mass flows do not occur because of the level controller.

---

The temperatures within the system are stabilized towards steady state. Yet, low values of  $T_{4x}$  below the dew point is experienced.

The 10% decrease in flue gas represented in Figure 4.10 lead to a decrease in the pressures and thus less power production. The lowered pressure increased the outlet temperature and thus the risk of condensation was not a problem for this case.

In the controlled case in Figure 4.22 the amount of decrease of  $\dot{m}_G$  during the simulation was limited by convergence of the solver and can thus be improved by a better model in the future. However, by analysing the plot we see that the pressures decrease with over 10% and thus lowering the power output substantially. It is also identified that the mass flow into the boiler decreases to stabilize the reduction of  $\dot{m}_2$  caused by the pressure drop. Larger decreases in the flue gas can therefore expect to lower the mass flows substantially and should also be considered a limitation. Thus, the step response with the added effect of the level and temperature controllers show a limitation for decreased values in flue gas as well, but the impacts are more with regards to power production and mass flow rates and not feasibility of the system.



## 6 — Conclusion

The first objective for this project was to model a simple steam cycle in Simulink and perform open loop responses. The second objective was to add a control structure, and with the use of several closed loop responses, study if the liquid holdup in the boiler could be used as an energy storage item to vary the power output for small periods of time, and within what limitations this can be done. Problems in the modelling of the mass flows by the linear valve equation lead to accumulation in the liquid holdup in the boiler and thus no proper steady state model was found for  $M_1$  at design conditions. It was however possible to tune and verify a level controller for  $M_1$ . For the temperature controller of  $T_2$  a 10% setpoint change indicated the need for a larger controller gain to obtain acceptable control.

The large liquid holdup before the turbine  $M_{turbine}$  slowed down the dynamics in the system and thus gave smooth responses, but also low sensitivity to the speed of the level controller. Still, the step responses indicate that an increase in the valve position,  $z$ , combined with an active level control could be used to produce higher power output for a short period of time. This effect can be increased by reducing the liquid holdups or lowering the level controller gain. The aim of using the liquid holdup as an energy storage cannot be concluded because of the instability in  $M_1$  itself, as well as inadequate coupling within its mass flows.

The Stodola approximation of the turbine flow was found to tolerate variations in the system better than using the constant volumetric flow approximation.

The variations in the flue gas was limited by +1% and -10%. This limitation was found to be mostly with regards to the increase in the flue gas as the computed temperature out of the turbine decreased below vaporization temperatures.



# Bibliography

- Faanes A. and Skogestad S. Buffer tank design for acceptable control performance. *Industrial & Engineering Chemistry Research*, 42(10):2198–2208, 2003. doi: 10.1021/ie020525v. URL <https://doi.org/10.1021/ie020525v>.
- Starkloff R. Lanz T. Heinze C. Alobaid F., Mertens N. and Epple B. Progress in dynamic simulation of thermal power plants. *Progress in Energy and Combustion Science*, 59:79 – 162, 2017. ISSN 0360-1285. doi: <https://doi.org/10.1016/j.pecs.2016.11.001>. URL <http://www.sciencedirect.com/science/article/pii/S0360128516300375>.
- D. H. Cooke. On prediction of off-design multistage turbine pressures by Stodola's ellipse. *Stone and Webster Engineering Corporation, Houston, TX*, 107:596–606, 1985.
- Himmelblau D.M. and Riggs J.B. *Basic Principles and Calculations in Chemical Engineering*. Always learning. Prentice Hall, 2012. ISBN 9780132346603. URL <https://books.google.no/books?id=Jk26u6f5-roC>.
- Rua Pazos J. Dynamic modeling and process simulation of steam bottoming cycle, 2017. URL <http://hdl.handle.net/11250/2454931>.
- J. Kovacs. Power plant control. *University of Oulu, Systems Engineering Laboratory*, pages 15–71, 2004-2014.
- Rech S. Mazzi N. and Lazzaretto A. Off-design dynamic model of a real organic Rankine cycle system fuelled by exhaust gases from industrial processes. *Energy*, 90:537 – 551, 2015. ISSN 0360-5442. doi: <https://doi.org/10.1016/j.energy.2015.07.083>. URL <http://www.sciencedirect.com/science/article/pii/S0360544215009780>.
- Skogestad S. Minasidis V. and Kaistha N. Simple rules for economic plantwide control. 37:101 – 108, 2015. ISSN 1570-7946. doi: <https://doi.org/10.1016/B978-0-444-63578-5.50013-X>. URL <http://www.sciencedirect.com/science/article/pii/B978044463578550013X>.
- Johnson M.A. Katebi R.M. Oryds A.W., Pike A.W. and Grimble M.J. 1994.
- Breeze P. Pushing the steam cycle boundaries, 2012. URL <https://doi.org/10.1016/j.pecs.2012.11.001>.

[//www.powerengineeringint.com/articles/print/volume-20/issue-4/features/pushing-the-steam-cycle-boundaries.html](http://www.powerengineeringint.com/articles/print/volume-20/issue-4/features/pushing-the-steam-cycle-boundaries.html).

Sinnott R. and Towler G. *Chemical Engineering Design*. ISBN 9780750685511.

Skogestad S. Simple analytic rules for model reduction and pid controller tuning. *Journal of Process Control*, 13(4):291 – 309, 2003. ISSN 0959-1524. doi: [https://doi.org/10.1016/S0959-1524\(02\)00062-8](https://doi.org/10.1016/S0959-1524(02)00062-8). URL <http://www.sciencedirect.com/science/article/pii/S0959152402000628>.

Skogestad S. and Grimholt C. *The SIMC Method for Smooth PID Controller Tuning*. Springer London, London, 2012. ISBN 978-1-4471-2425-2. doi: 10.1007/978-1-4471-2425-2\_5. URL [https://doi.org/10.1007/978-1-4471-2425-2\\_5](https://doi.org/10.1007/978-1-4471-2425-2_5).

S. Skogestad. Simple analytic rules for model reduction and pid controller tuning. pages 291–309, 2004.

S. Skogestad. *Prosessteknikk Masse- og energibalanser*. Tapir akademisk forl., 2009.

Inc The MathWorks. Solve differential algebraic equations (daes), 2018a. URL <https://nl.mathworks.com/help/matlab/math/solve-differential-algebraic-equations-daes.html>.

Inc The MathWorks. Model differential algebraic equations, 2018b. URL <https://nl.mathworks.com/help/simulink/ug/model-a-differential-algebraic-equation.html#bub3i22-1>.

Inc The MathWorks. Simulink, 2018c. URL <https://nl.mathworks.com/help/simulink/>.

# A — Appendix

## A.1 Units

The symbol and units used for the respected quantities are listed in Table A.1 below.

Quantity	Symbol	SI Units
Mass	M	kg
Enthalpy	H	J
Specific enthalpy	h	$Jkg^{-1}$
Temperature	T	K
Heat flow	Q	$Js^{-1}$
Pressure	P	Pa
Mass flow	$\dot{m}$	$kg s^{-1}$
Volumetric flow rate	q	$m^3 s^{-1}$
Universal gas constant	R	$Jmol^{-1}K^{-1}$
Molar mass	Mm	$kgmol^{-1}$
Volume	V	$m^3$
Heat capacity	$C_p$	$Jkg^{-1}K^{-1}$
Heat of vaporization	$\Delta_{vap}H$	$Jkg^{-1}$
Heat transfer coefficient multiplied with the surface area	UA	$Wm^{-2}K^{-1}$
Valve coefficient	$K_v$	$kgPa^{-1}s^{-1}$

**Table A.1:** Symbols and SI units for the quantities in the steam cycle

Quantity	Unit	Conversion factor to SI units
P	Bar	$10^5$ Pa
T	°C	$T + 273.15$ K

**Table A.2:** SI unit conversion table

## A.2 Parameters

The parameters used for the simulation are listed in Table A.3

Parameter	Symbol	Value	Units
Volumetric flow	$q$	0.2488	$m^3 s^{-1}$
Universal gas constant	$R$	8.3145	$J mol^{-1} K^{-1}$
Molar mass of water	$Mm_{water}$	18e-3	$kg mol^{-1}$
Volume in the attemperator	$V_{mix}$	10	$m^3$
Volume in the turbine	$V_{turbine}$	10	$m^3$
Specific heat capacity of steam	$C_{p,steam}$	2000	$J kg^{-1} K^{-1}$
Sepecific heat capacity of the flue gas	$C_{p,gas}$	3000	$J kg^{-1} K^{-1}$
Turbine outlet pressure	$P_4$	0.096e5	Pa
Pump outlet pressure	$P_0$	130e5	Pa
Boiler and bypass initial temperature	$T_0$	318.15	K
Heat of vaporization for water at $T_{ref} = 45^\circ C$	$\Delta_{vap}H$	2.4e6	$J kg^{-1}$
UA for the HEX in the boiler	$UA_1$	1.6605e+05	$W m^{-2} K^{-1}$
UA for the HEX in the superheater	$UA_2$	7.6121e+03	$W m^{-2} K^{-1}$
UA for the HEX in the reboiler	$UA_3$	5.1290e+03	$W m^{-2} K^{-1}$
Valve coefficient for $m_2$	$K_{v,m_2}$	4.6141e-05	$kg Pa^{-1} s^{-1}$
Valve coefficient for $m_3$	$K_{v,m_3}$	1.3806e-05	$kg Pa^{-1} s^{-1}$
Valve coefficient for $m_4$	$K_{v,m_4}$	-4.8030e-07	$kg Pa^{-1} s^{-1}$

**Table A.3:** Parameter values

### A.3 Steady state data and nominal values

The steady state data (initial values) and nominal values used in the simulation are rendered in Table A.4 and A.5 below.

State	Steady state values	Units
$M_1$	1000	kg
$H_1$	2.9319e9	J
$T_1$	584.0833	K
$M_{mix}$	253	kg
$T_2$	802.1171	K
$P_2$	9.8001e6	Pa
$M_{turbine}$	1000	kg
$P_3$	9.2919e6	Pa
$M_c$	983.8729	kg
$M_s$	90.1090	kg
$T_{G2}$	272.5266	K
$Q_1$	1.7515e7	$J s^{-1}$
$T_{G1}$	1.1055e3	K
$Q_2$	3.4973e6	$J s^{-1}$
$T_{2hot}$	876.7845	K
$T_{3mid}$	613.8158	K
$T_{G3}$	1.0975e3	K
$Q_3$	3.6894e6	$J s^{-1}$

**Table A.4:** Table with the steady state data for the steam cycle states

Input	Nominal value	Units
$\dot{m}_1$	5.975	$kg s^{-1}$
$\dot{m}_2$	5.975	$kg s^{-1}$
$\dot{m}_{bypass}$	0.2649	$kg s^{-1}$
$z$	0.8911	-
$Q_c$	-14976e7	$J s^{-1}$
$\dot{m}_G$	7	$kg s^{-1}$
$\dot{m}_{G2}$	7	$kg s^{-1}$

**Table A.5:** Nominal values used in the simulation for the respected steam cycle inputs

## A.4 Setpoints for the PID controllers

State	Setpoint	Unit
$M_1$	1000	kg
$T_2$	802	K
$P_1$	9.9241e6	Pa
$W_s$	-9.7222e6	W
$T_{3mid}$	613.9	K
$T_4$	318.15	K

**Table A.6:** The desired setpoints used in the closed controller loop for the respected PID controllers

## A.5 Step responses for tuning of controller

Open loop step responses was made for each of the control pairings to tune the controllers with the use of the SIMC tunings. A subsequent closed loop setpoint change in the setpoints were made to verify the respected controller tunings.

### A.5.1 Holdup controller of $M_1$

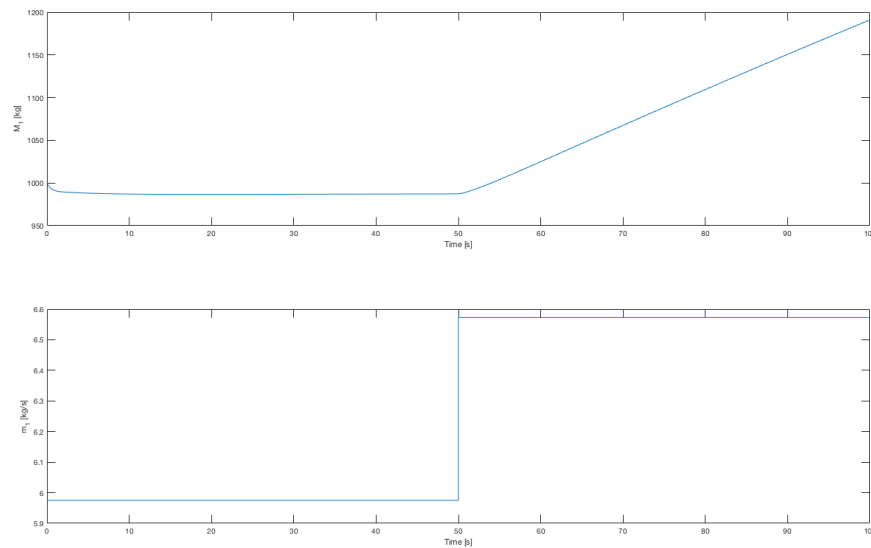


**Figure A.1:** Plot of  $M_1$  and  $\dot{m}_1$  after a 10% open loop step response in  $\dot{m}_1$

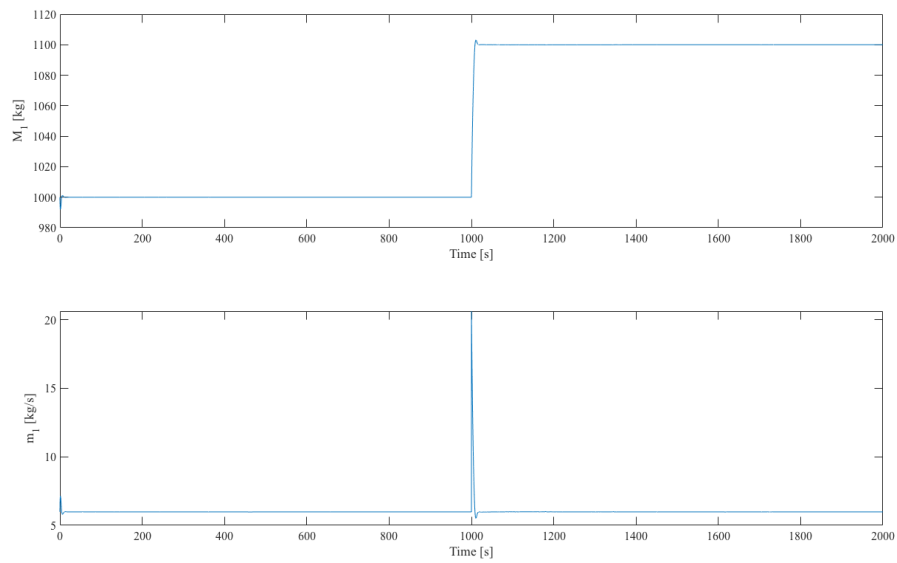


**Figure A.2:** Plot of  $M_1$  and  $\dot{m}_1$  after a 10% closed loop setpoint changer in  $M_{1s}$ .  $K_{c1} = 0.1465$

### A.5.2 Temperature controller of $T_2$

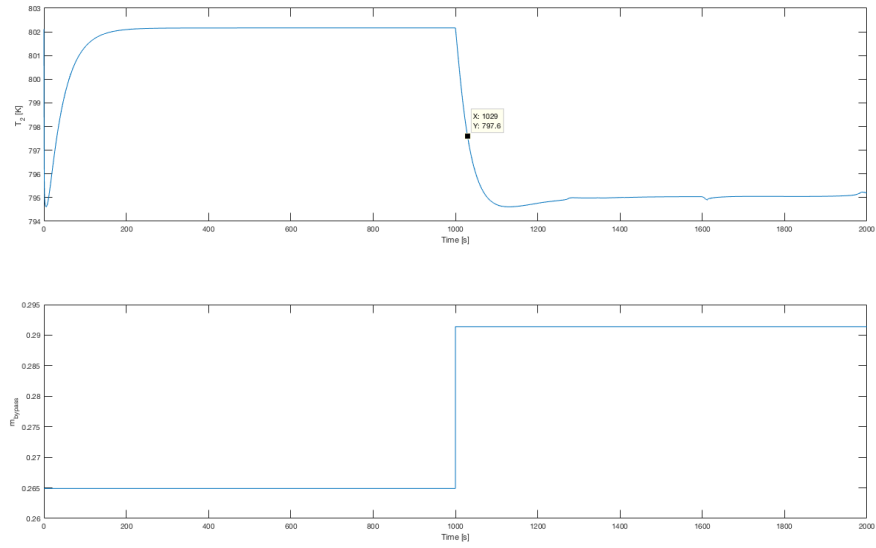


**Figure A.3:** Plot of  $T_2$  and  $\dot{m}_{bypass}$  after a 10% open loop step response in  $\dot{m}_{bypass}$

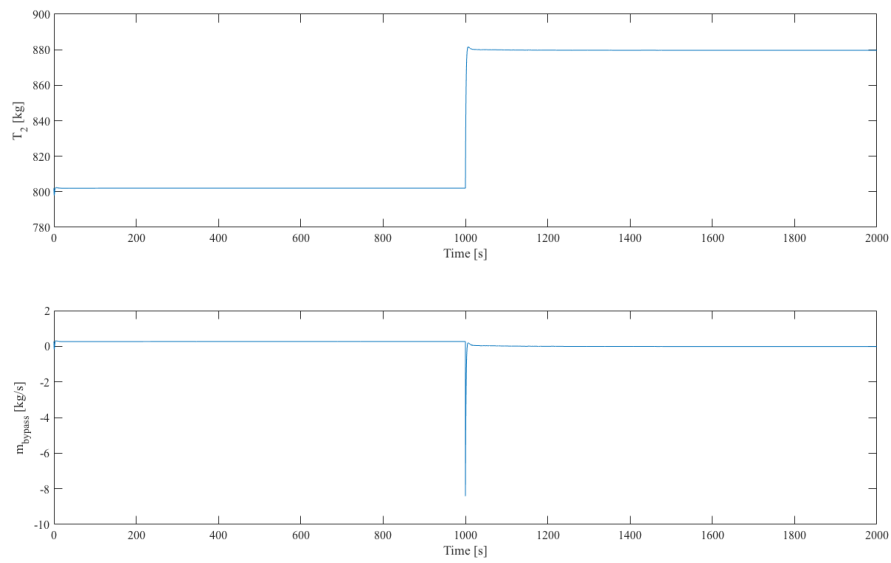


**Figure A.4:** Plot of  $T_2$  and  $\dot{m}_{bypass}$  after a 10% closed loop setpoint change in  $T_2$ .  $K_{cbypass} = -0.1082$

### A.5.3 Temperature controller of $T_{3mid}$

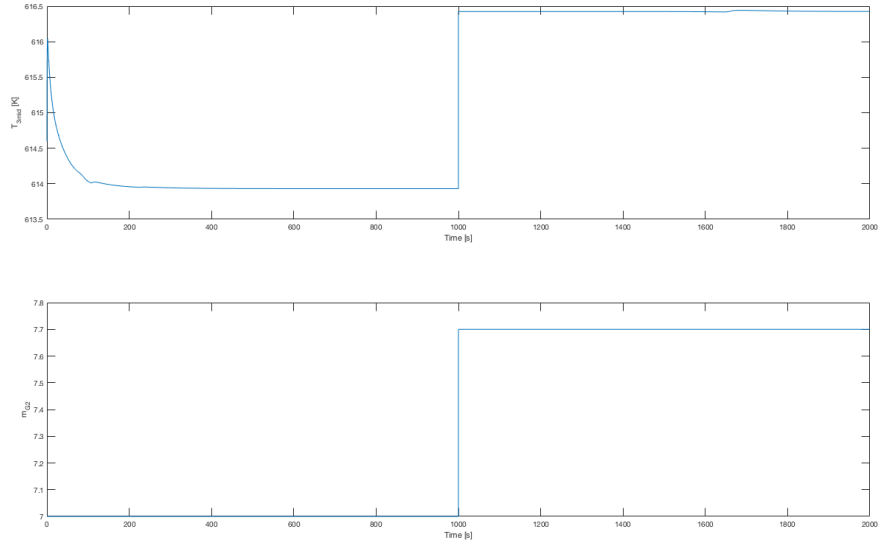


**Figure A.5:** Plot of  $T_{3mid}$  and  $\dot{m}_{G2}$  after a 10% open loop step response in  $\dot{m}_{mG}$

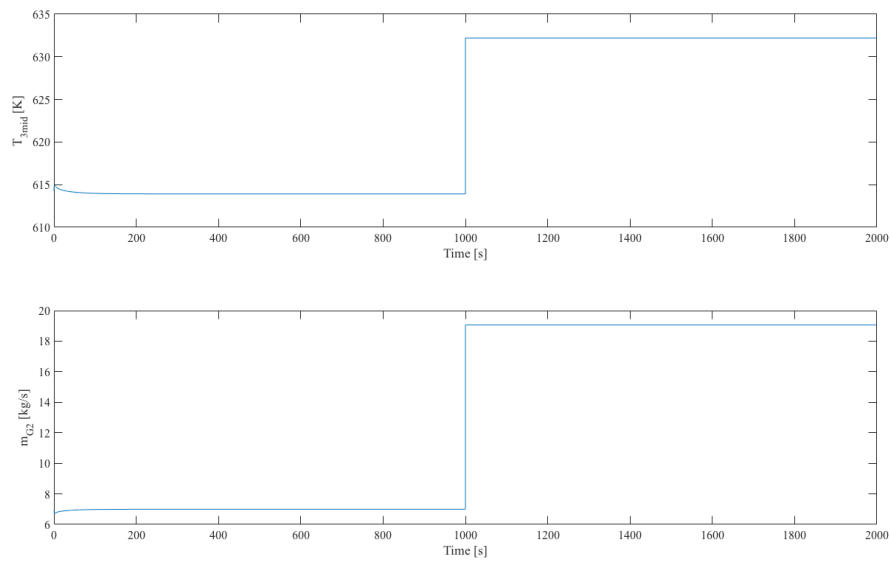


**Figure A.6:** Plot of  $T_{3mid}$  and  $\dot{m}_{G2}$  after a 10% closed loop setpoint change in  $T_{3mids}$ .  
 $K_{cReheater} = 0.28$

### A.5.4 Temperature controller of $T_4$

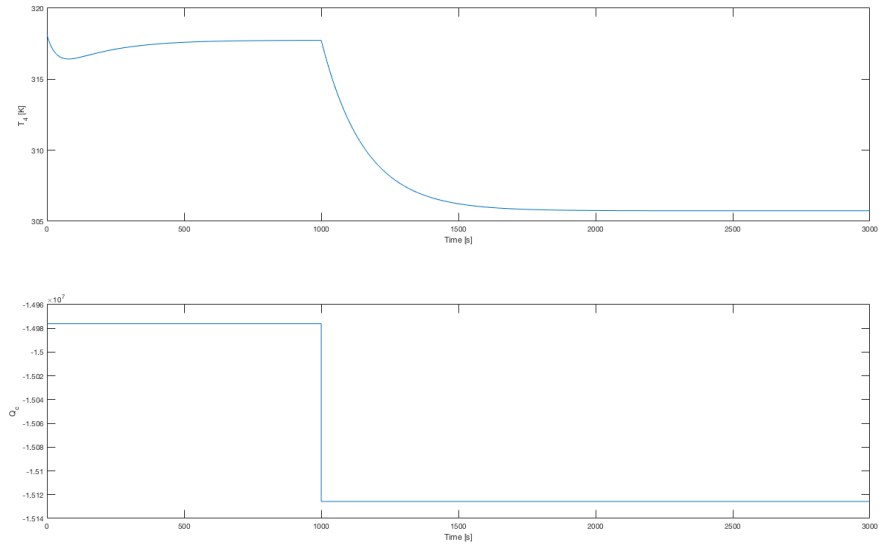


**Figure A.7:** Plot of  $T_4$  and  $Q_c$  after a 10% open loop step response in  $Q_c$

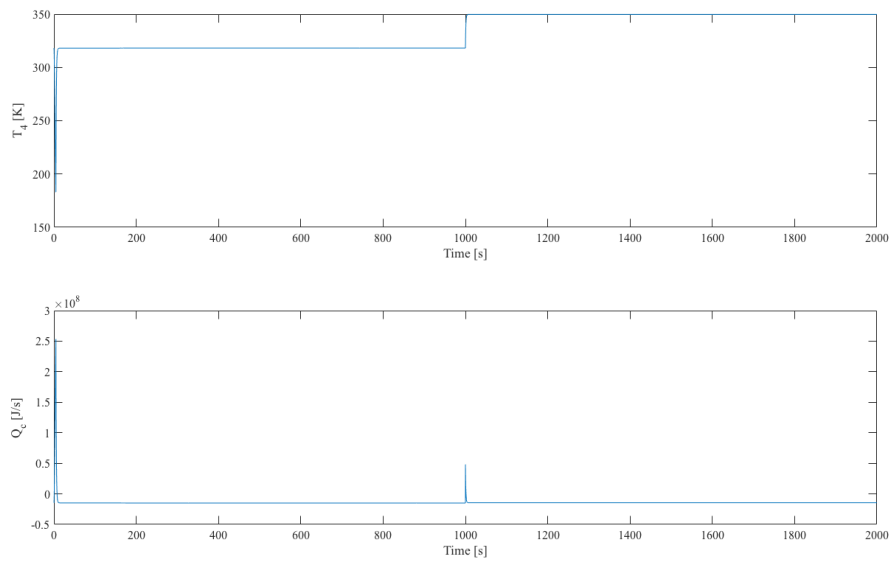


**Figure A.8:** Plot of  $T_4$  and  $Q_c$  after a 10% closed loop closed loop setpoint change in  $T_{4s}$ .  
 $K_{cQc} = 1.9843e6$

### A.5.5 Pressure controller of $P_1$

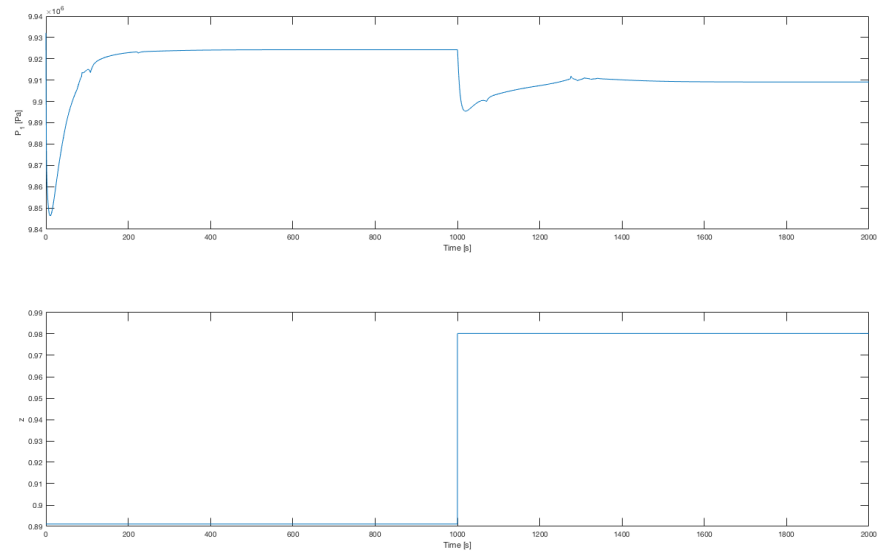


**Figure A.9:** Plot of  $P_1$  and  $z$  after a 10% open loop step response in  $z$

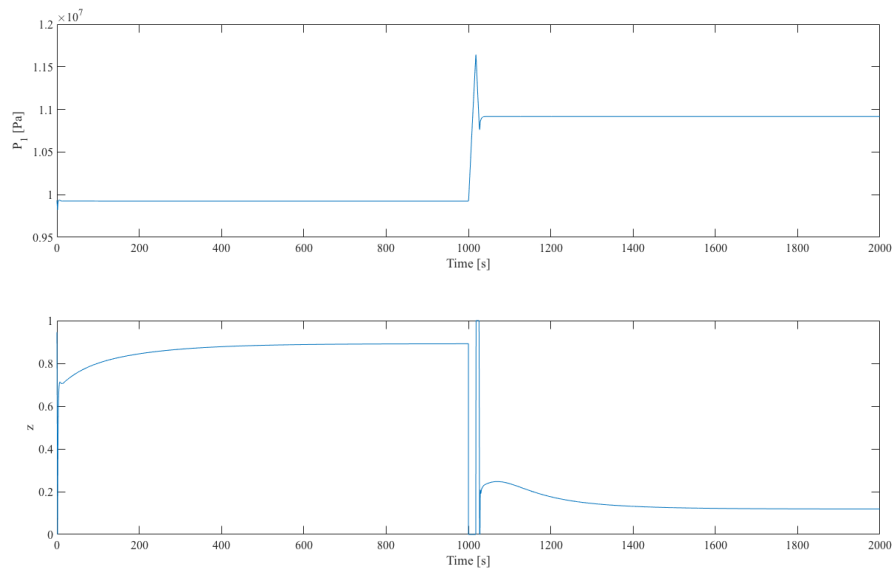


**Figure A.10:** Plot of  $P_1$  and  $z$  after a 10% closed loop setpoint change in  $P_{1s}$ .  $K_{cz} = -6.8538e-06$ ,  $\tau_{Iz} = 3$

### A.5.6 Power controller of $W_s$

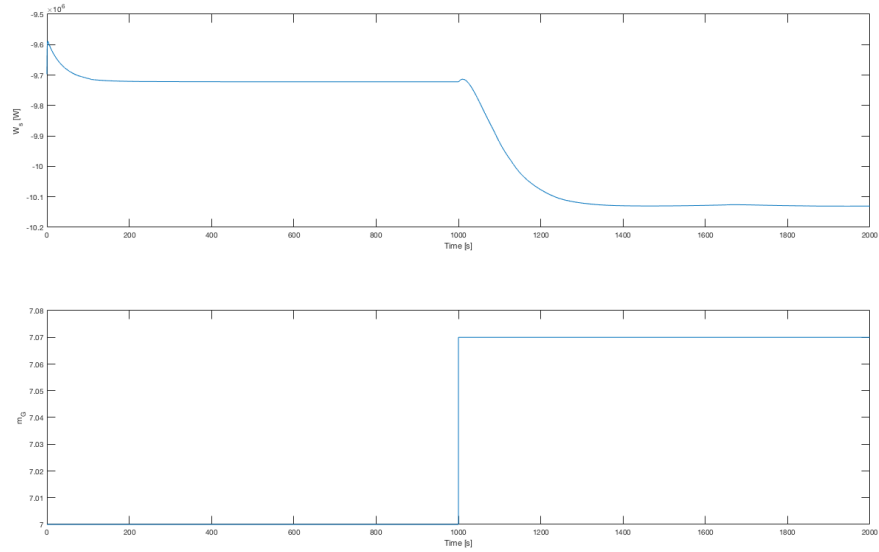


**Figure A.11:** Plot of  $W_s$  and  $\dot{m}_G$  after a 1% open loop step response in  $\dot{m}_G$

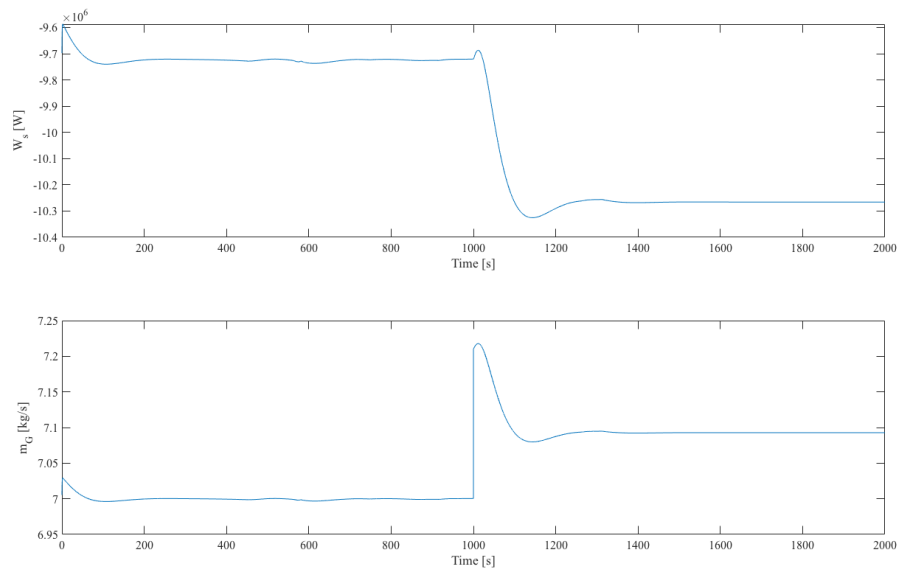


**Figure A.12:** Plot of  $W_s$  and  $\dot{m}_G$  after a 1% closed loop setpoint change in  $W_s$ .  $K_{cW_s} = -2.1620e-7$

## A.6 Step responses with holdup control (MC)

The Holdup controller for  $M_1$  was activated and step responses for the bypass flow, valve position and flue gas flow was made. The plots are with intermediate holdup controller,  $K_{c1} = 0.1465$  if not otherwise specified.

### A.6.1 Increase in bypass flow

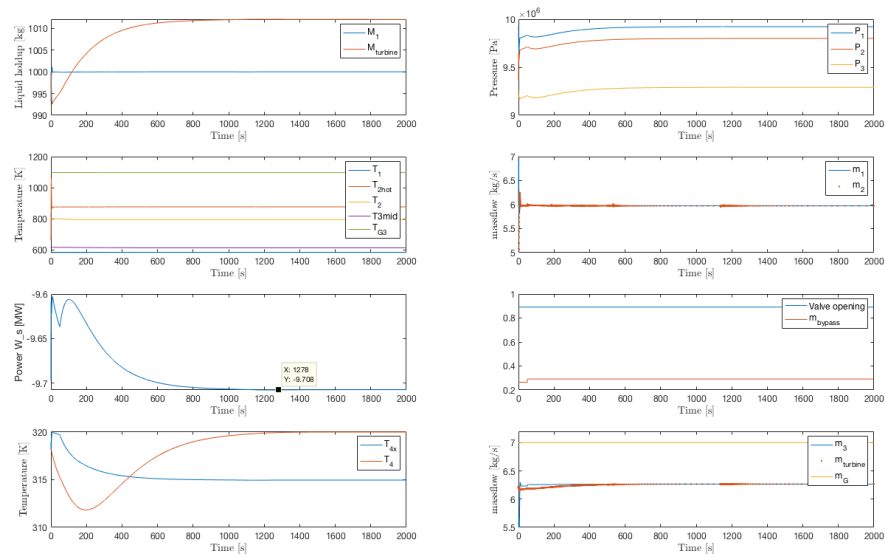


Figure A.13: Plot of the response after a 10% step of  $\dot{m}_{bypass}$  with MC on

### A.6.2 Variation of valve position

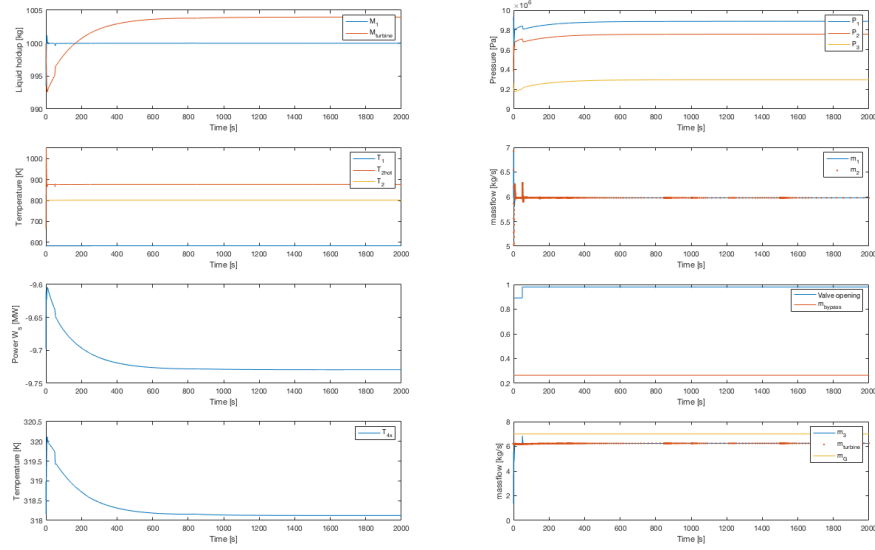


Figure A.14: Plot of the response after a 10% step of  $z$  with MC on.  $Kc1 = 0.1465$

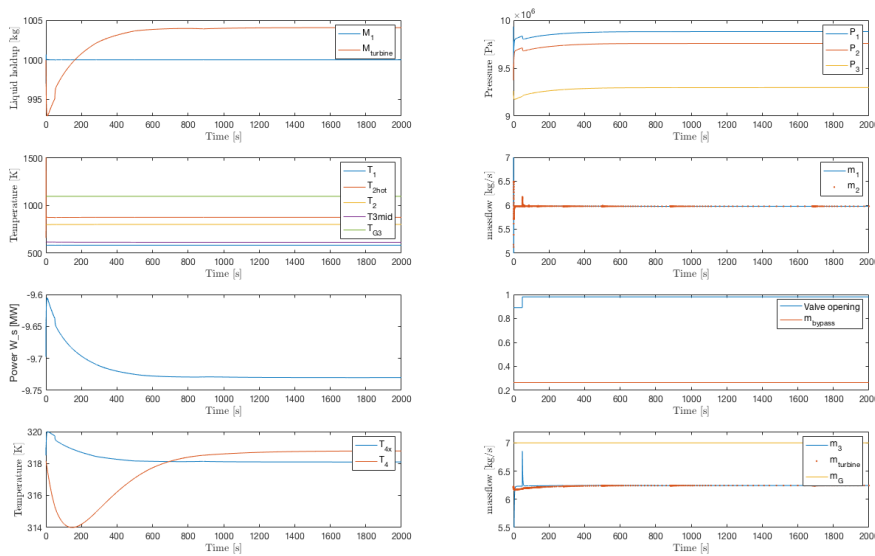


Figure A.15: Plot of the response after a 10% step of  $z$  with MC on.  $Kc1 = 1.465$

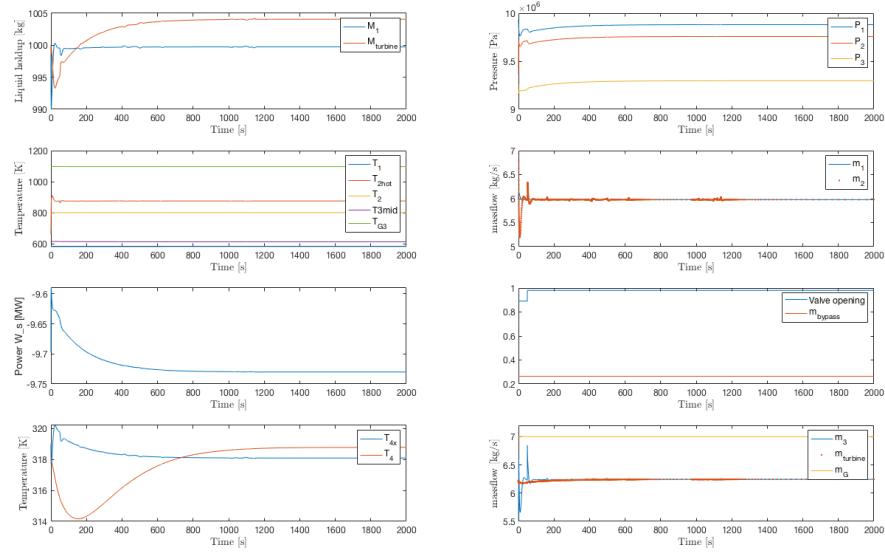


Figure A.16: Plot of the response after a 10% step of  $z$  with MC on.  $Kc1 = 14.65$

### A.6.3 Variation of flue gas flow in HEX

The flow of the flue gas in the HEX was varied to check for limitations on how much it can vary before causing instability or unfeasible conditions.

#### Increase in $\dot{m}_G$

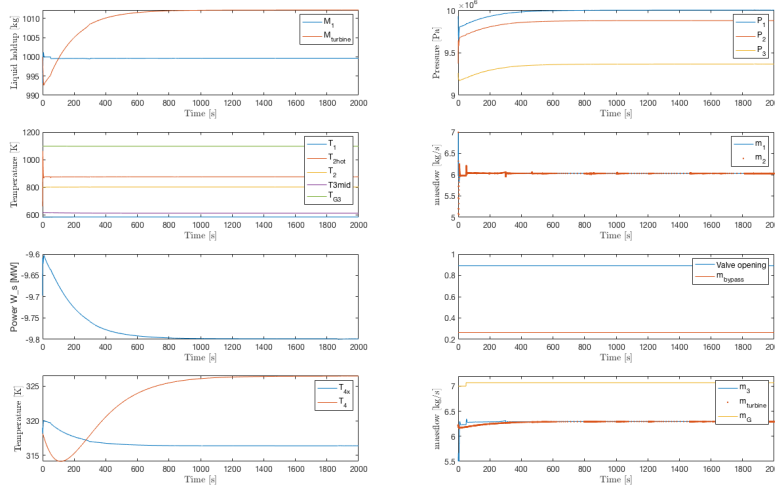


Figure A.17: Plot of the response after a 1% step of  $\dot{m}_G$  with MC on.  $Kc1 = 0.1465$

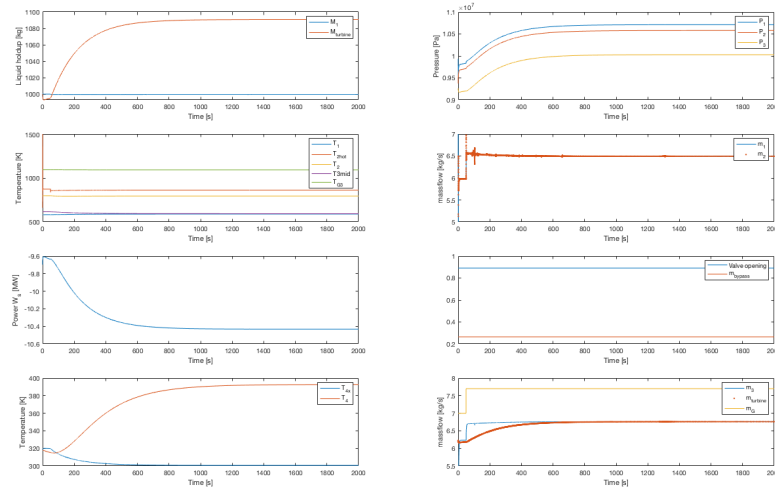


Figure A.18: Plot of the response after a 1% step of  $\dot{m}_G$  with MC on.  $Kc1 = 14.65$

Decrease in  $\dot{m}_G$

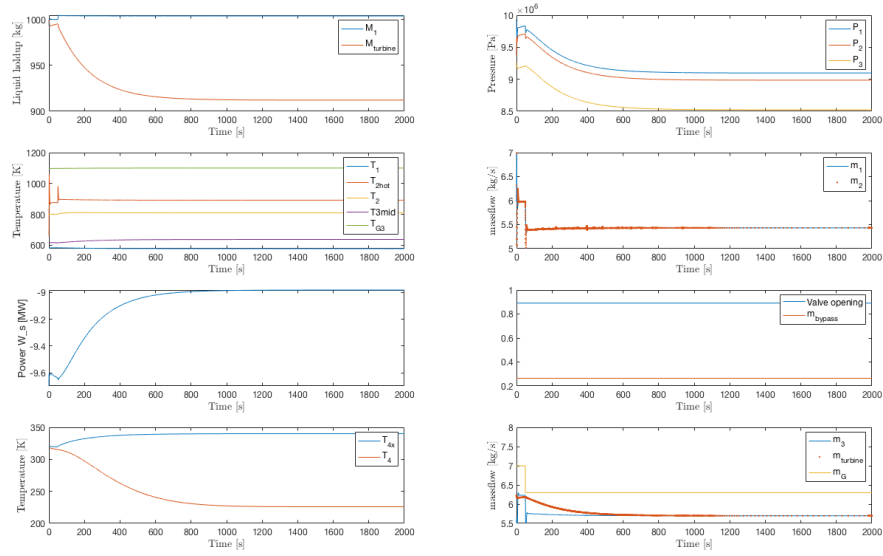


Figure A.19: Plot of the response after a -10% step of  $\dot{m}_G$  with MC on.  $Kc1 = 0.1465$

## A.7 Figure of the Simulink model

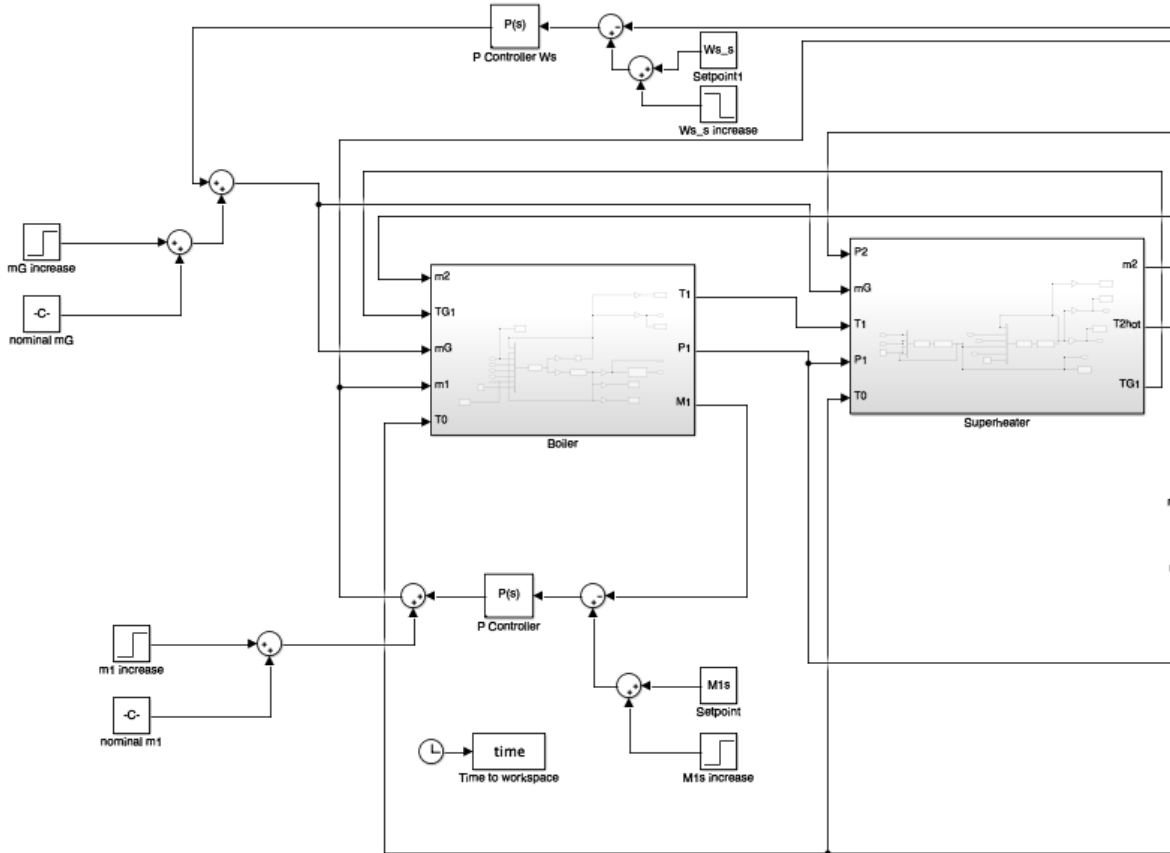


Figure A.20: Screen-shot of the steam cycle Simulink model part 1

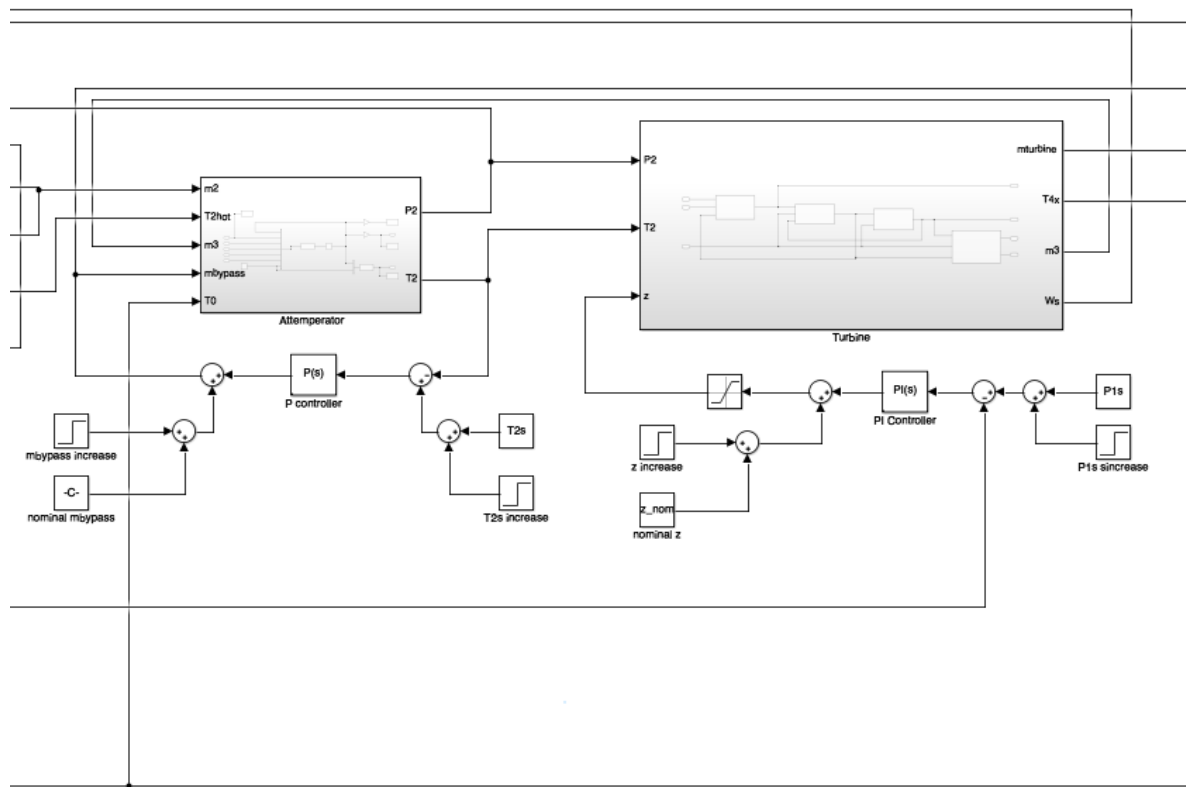


Figure A.21: Screen-shot of the steam cycle Simulink model part 2

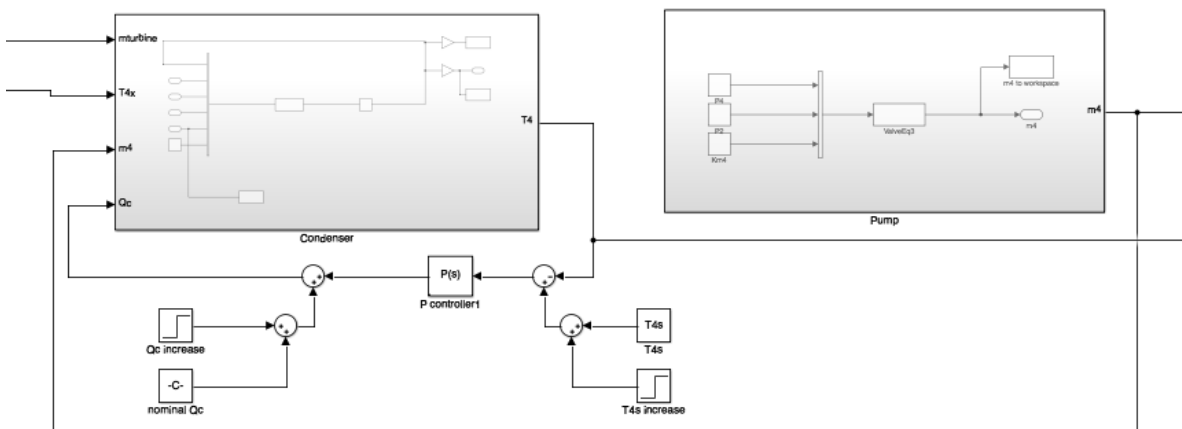
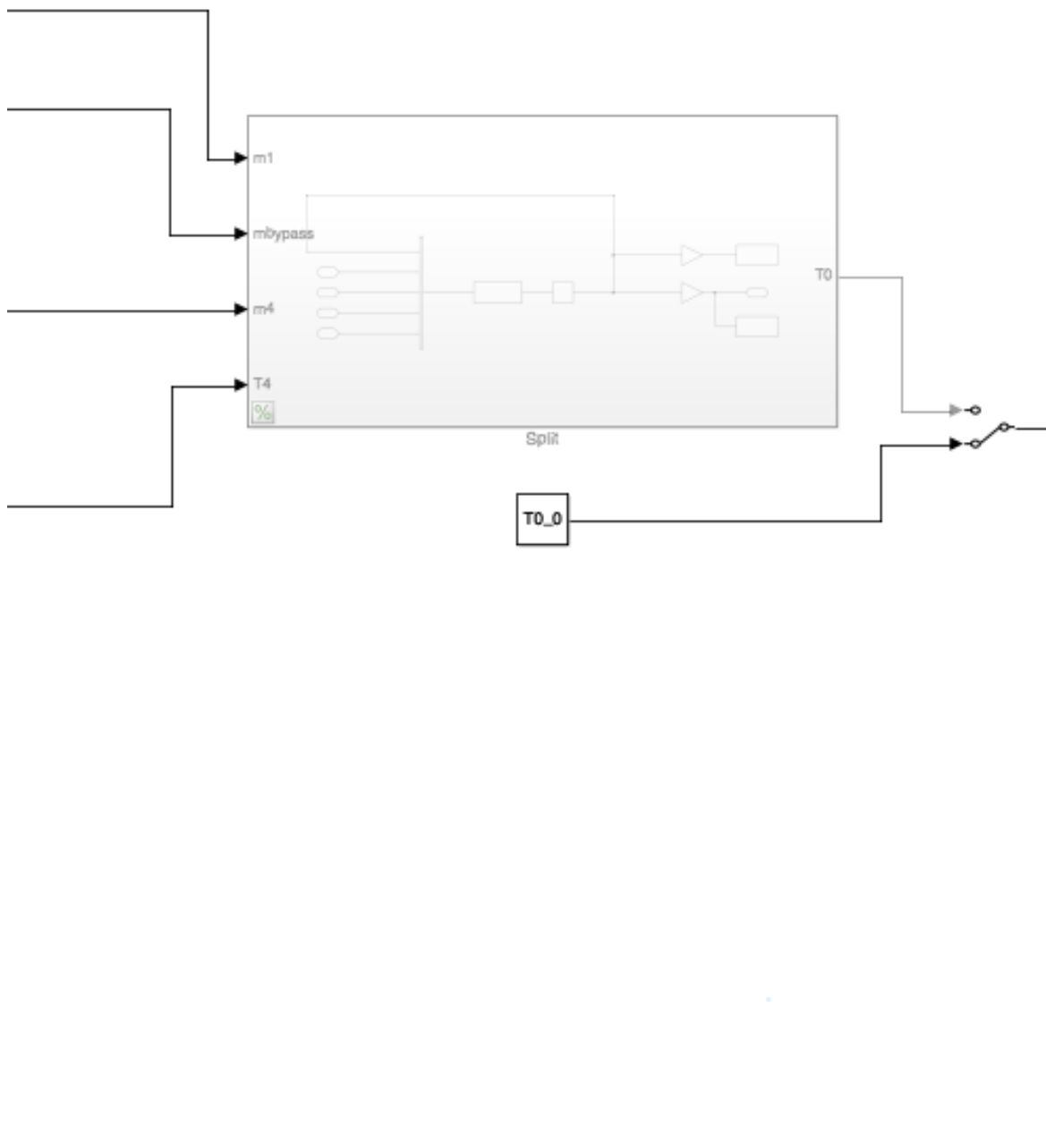


Figure A.22: Screen-shot of the steam cycle Simulink model part 3



**Figure A.23:** Screen-shot of the steam cycle Simulink model part 4